

GEOTECHNICAL ENGINEERING
RESEARCH ON STRENGTH-DEFORMABILITY-WATER PRESSURE
RELATIONSHIPS FOR FAULTS IN DIRECT SHEAR

AD 747673

by

R. E. Goodman

F. E. Heuzé

Y. Ohnishi

D D C
RECEIVED
SEP 5 1972
RELATIVE
D.

Final Report on ARPA Contract H0210020 - Amount \$ 44,701

Effective Date : February 5, 1972

Termination Date : March 5, 1972

Principal Investigator : Prof. R.E. Goodman (415) 642-5525

Faculty Investigator : Dr. F.E. Heuzé (415) 642-4217

Sponsored by Advanced Research Projects Agency
ARPA Order No. 1579-Amend.2-Program Code No. 1F10

APRIL 1972

DISTRIBUTION STATEMENT 1

Approved for public release;
Distribution Unlimited

UNIVERSITY OF CALIFORNIA • BERKELEY

Reproduced by
NATIONAL TECHNICAL
INFORMATION SERVICE
U S Department of Commerce
Springfield VA 22151

RESEARCH ON STRENGTH-DEFORMABILITY-WATER PRESSURE
RELATIONSHIPS FOR FAULTS IN DIRECT SHEAR

Final Report on ARPA Contract H0210020

ERRATA SHEET

<u>Page</u>	<u>Line</u>	
1 & 52	20	After rock types insert, <u>except for granite at high roughnesses</u>
1 & 52	26	Change <u>an increase</u> to <u>a decrease</u>
3	19	Change <u>532</u> to <u>360</u>
13	6	Change <u>4, 5, and 6</u> to <u>7, 8, and 9</u>
41	16	Change <u>except at high values (say >10)</u> to <u>at low normal stress values</u>
42	9 & 10	Change <u>3</u> to <u>2</u>
	12	Change <u>4</u> to <u>3</u>
	15	Insert <u>normal</u> before pressure
	15	The portion after the semicolon should read <u>the primary factor influencing δ is R</u>
43	10	Delete <u>and</u>
	12	Should read <u>the no-dilation normal pressure is in excess of 1,500 psi</u>
45	21	Change <u>consistently</u> to <u>usually</u>

Mar 7, 66

Security Classification

DOCUMENT CONTROL DATA - R & D

(Security classification of title, body of abstract and indexing annotation must be entered when the overall report is classified)

1. ORIGINATING ACTIVITY (Corporate author)		2a. REPORT SECURITY CLASSIFICATION	
Geological Engineering University of California, Berkeley		Unclassified	
3. REPORT TITLE		7b. GROUP	
Research on Strength-Deformability-Water pressure Relationships for Faults in Direct Shear.			
4. DESCRIPTIVE NOTES (Type of report and inclusive dates)			
Final Report February 5, 1971 - March 5, 1972			
5. AUTHOR(S) (First name, middle initial, last name)			
R.E. Goodman, F.E. Heuzé, Y. Ohnishi			
6. REPORT DATE		7a. TOTAL NO. OF PAGES	7b. NO. OF REFS
April 1972		81	5
8a. CONTRACT OR GRANT NO.		9a. ORIGINATOR'S REPORT NUMBER(S)	
b. PROJECT NO.			
c.		9b. OTHER REPORT NO.'S (Any other numbers that may be assigned this report)	
d.			
10. DISTRIBUTION STATEMENT			
Distribution of this report is unlimited			
11. SUPPLEMENTARY NOTES		12. SPONSORING MILITARY ACTIVITY	
		Military Geophysics Program. Advanced Research Projects Agency	
13. ABSTRACT			
<p>A program of direct shear tests on samples of rock joints was initiated to gain an improved picture of the deformation and strength of jointed rock masses under load. The shear testing machine, developed under an NSF grant, and improved during this project, allows water pressure to be monitored in the joint plane during shearing. Seventy-two tests were conducted in this first year of an intended 3 year's program; artificial joints were created in two rock types--granite and sandstone-- with varying wall roughness, filling material thickness, and environmental conditions.</p> <p>Joints and faults exert controls on rock movement below ground and their weakness and deformability limit the "hardness" of underground sites. Furthermore, water pressure phenomena create difficulties for design and construction. This research has added to the technology basis to rational engineering with rock masses. In the work, basic phenomena of jointed rock are being examined experimentally for the first time permitting formulation of correct constitutive laws for joints that are vital to numerical and physical modelling. In continuation, tests with jacketed specimens having preconsolidated filler material are proposed. Experimental methods for these improvements in testing technique have now been developed.</p>			

DD FORM 1473
NOV 66Unclassified
Security Classification

A

Security Classification

14. KEY WORDS	LINK A		LINK B		LINK C	
	ROLL	WT	ROLL	WT	ROLL	WT
Direct Shear Tests						
Faults						
Granite						
Gouge Material						
Joint Dilatancy						
Joint Roughness						
Joint Stiffness						
Joint Strength						
Joint Waviness						
Kaolinite						
Sandstone						
Water Pressure						

Unclassified

Security Classification

B

Geotechnical Engineering

RESEARCH ON STRENGTH-DEFORMABILITY-WATER PRESSURE
RELATIONSHIPS FOR FAULTS IN DIRECT SHEAR

by

R. E. Goodman
F. E. Heuzé
Y. Ohnishi

Final Report - Contract ARPA No. H0210020 - Amount \$44,701
Effective Date: February 5, 1971 - Termination Date: March 5, 1972

Principal Investigator: Professor R. E. Goodman (415) 642-5525
Co-Investigator: Dr. F. E. Heuzé (415) 642-5525

Sponsored by Advanced Research Projects Agency
ARPA Order No. 1579 - Amend. 2 - Program Code 1F10

Monitored by U.S. Bureau of Mines; T. Bur Project Officer

The views and conclusions contained in this document are those of the authors and should not be interpreted as necessarily representing the official policies either expressed or implied of the Advanced Research Projects Agency or the U. S. Government.

April 1972

University of California, Berkeley

SUMMARY OF TECHNICAL REPORT

A program of direct shear tests on samples of rock joints was initiated to gain an improved picture of the deformation and strength of jointed rock masses under load. The shear testing machine, developed under an NSF grant, and improved during this project, allows water pressure to be monitored in the joint plane during shearing. Seventy-two tests were conducted in this first year of an intended 3 year's program; artificial joints were created in two rock types -- granite and sandstone -- with varying wall roughness, filling material thickness, and environmental conditions.

The methods of preparing joint specimens of varying roughness were developed in this project; rough artificial joints were manufactured by splitting the specimens and smooth joints by diamond sawing and lapping. It was difficult to fill the joints to a predetermined thickness with gouge preconsolidated to a desired high normal pressure; remoulded gouge was therefore introduced. Roughness measurements were made and statistical parameters of roughness and waviness were computed using two specially written programs to be found in Appendices B and C. Typical test records are also given in the Appendix.

Table 7 summarizes the sensitivity of deformability and strength parameters to the variables studied. For the sandstone and granite specimens, both peak displacement and joint stiffness varied with normal pressure. The dilation angle decreased rapidly with normal pressure for both rock types and became negative for the sandstone specimens at σ above 500 psi (i.e. the specimens contracted during shear). Induced water pressures measured were not large (<25 psi), possibly due to the problem of sampling water pressures in the joint plane, partly due to the remoulded nature of the filling, and partly because of decay of the water pressure transients in theunjacketed specimens. Dilatant joints generally suffered an increase in pressure while contractant joints underwent a pore pressure buildup. Complete saturation of the joints was obtained, as

evidenced by the insensitivity of the results to chamber back pressure. Filled joints approached the strength of the clay filling material when the thickness was greater than about 3 times the mean roughness amplitude.

Joints and faults exert controls on rock movement below ground and their weakness and deformability limit the "hardness" of underground sites. Furthermore, water pressure phenomena create difficulties for design and construction. This research has added to the technology basic to rational engineering with rock masses. In the work, basic phenomena of jointed rock are being examined experimentally for the first time permitting formulation of correct constitutive laws for joints that are vital to numerical and physical modelling. In continuation, tests with jacketed specimens having preconsolidated filler material are proposed. Experimental methods for these improvements in testing technique have now been developed.

PREFACE

This research was conducted by the Geological Engineering Group of the University of California, Berkeley. The Principal Investigator was Dr. Richard E. Goodman, Associate Professor of Geological Engineering. Co-Investigator was Dr. Francois E. Heuzé, Lecturer and Assistant Research Engineer in Geological Engineering. They were assisted by Mr. Yuzo Ohnishi, Research Assistant, to plan, perform and analyze the test program.

Additional personnel who contributed to this research are Mr. Quentin Gorton who developed and modified testing equipment in the first part of the research, assisted by Mr. John Walsh, and Mr. Mariano de Angulo who conducted studies of filler material consolidation and pore pressure development in clay material.

Miss Wanda Brandon typed the manuscript.

INDEX

	<u>Page</u>
SUMMARY OF TECHNICAL REPORT	i
PREFACE	iii
LIST OF FIGURES	vi
LIST OF TABLES	vii
 <u>PART I: INTRODUCTION - OBJECTIVES</u>	
1. NATURE OF THE PROGRAM	1
2. PRINCIPLES INVOLVED - JOINT MECHANICS	1
a. The Direct Shear Test for Rock Joints	
b. Parameters of Joint Behavior	
3. PROGRAM PLAN AND VARIABLES	3
 <u>PART II: METHOD OF INVESTIGATION</u>	
1. EQUIPMENT	12
2. SPECIMEN PREPARATION	13
a. Cutting and Potting	
b. Roughness and Waviness Measurements	
c. Filling Material	
3. TESTING PROCEDURE	15
4. PRACTICAL DIFFICULTIES	16
a. Jacketing of Specimens	
b. Water Pressure Measurement	
c. Filler Material	
d. Normal Stiffness Measurements	
 <u>PART III: RESULTS OF THE TEST PROGRAM</u>	
1. PROPERTIES OF THE "GRANITE" AND THE SANDSTONE	28
a. Petrographic Examination	
b. Strength-Deformability and Bulk Properties	
2. ROUGHNESS AND WAVINESS OF THE JOINT PLANES	28
a. Roughness	
b. Waviness	
3. THICKNESS OF JOINT FILLER	28
4. DEFORMABILITY AND STRENGTH DATA	29
5. WATER PRESSURE DATA	30

Index (Continued)

PagePART IV: DISCUSSION OF THE TEST RESULTS

1. DISCUSSION OF JOINT DEFORMABILITY	41
a. Sandstone Joints	
b. Granite Joints	
2. DISCUSSION OF JOINT STRENGTH	43
3. DISCUSSION OF WATER PRESSURE RESULTS	45

PART V: SUMMARY-CONCLUSIONS

REFERENCES	54
APPENDIX A - PETROGRAPHY AND MINERALOGY OF THE PROJECT'S ROCK TYPES	55
APPENDIX B - ROUGHNESS ANALYSIS PROGRAM, AND SAMPLE OUTPUT FOR TEST #61	60
APPENDIX C - WAVINESS ANALYSIS PROGRAM, AND SAMPLE OUTPUT FOR TEST #61	68
APPENDIX D - TYPICAL TEST RECORD (TEST #61)	74
APPENDIX E - DOD DOCUMENT CONTROL DATA - R & D	79

LIST OF FIGURES

	<u>Page</u>
FIG. 1 Normal displacement of discontinuity under changing normal stress with constant shear stress	9
FIG. 2 Shear displacement under changing shear stress with constant normal stress	10
FIG. 3b Actual dilation rates at different normal stresses	11
FIG. 4 36-Inch saw assembly	19
FIG. 5 Drill and vise assembly	20
FIG. 6 Roughness measuring system on mill table	21
FIG. 7 Direct shear machine, top removed	22
FIG. 8 Shear testing assembly and controls	23
FIG. 9 Normal loading device and regulator system	24
FIG. 10 Electronic data recording system	25
FIG. 11 Outline of testing procedure for direct shear tests	26
FIG. 12 Shear specimen assembled for testing (legend in text)	27
FIG. 13 Half specimen lay-out for roughness measurement	27
FIG. 14 Roughness distribution of sandstone joints	38
FIG. 15 Roughness distribution of granite joints	38
FIG. 16 Average slope angle vs. length of observation on joint planes	39
FIG. 17 Maximum positive slope angle vs. roughness of joint planes	39
FIG. 18 Dimensionless filler thickness (T_f/R) for sandstone joints	40
FIG. 19 Dimensionless filler thickness for granite joints	40
FIG. 20 Peak strength of sandstone specimens	47
FIG. 21 Residual strength of sandstone specimens	48
FIG. 22 Peak strength of wet granite specimens	49
FIG. 23 Residual strength of wet granite	50
FIG. 24 Strength data for clay filled joints	51
FIG. 25 Record of test #61	78

LIST OF TABLES

	<u>Page</u>
TABLE 1: The test program	4
TABLE 2: Number of tests on each rock type used to analyze the influence of the various parameters, on the strength and deformability of the joints	8
TABLE 3: Summary of index properties for the rock types of the shear program	31
TABLE 4: Strength and deformability data for tests of the shear program	32
TABLE 5: Normal stiffness values for selected tests on filled joints	30
TABLE 6: Water pressures observed for tests on sandstone and granite joints	35
TABLE 7: Influence of the test program variables on joint deformability parameters	37

PART I: INTRODUCTION - OBJECTIVES

1. NATURE OF THE PROGRAM

The manner and rate of rock movements virtually control the cost of excavation, support, and operation underground. Rock movements, in turn, are largely dictated by the behavior of seams, joints, and faults which tend to destroy continuity of the rock mass. Methods of physical model study and finite element analysis make it possible to simulate the behavior of discontinuities in an engineering study of a particular underground scheme. However, very little is known about the relevant properties of the seams and joints. Existing knowledge on the methods of sampling and testing discontinuities in the laboratory and in the field was recently summarized by Goodman, (1970). The state of knowledge is unsatisfactory in that almost no attention has been paid to the development of water pressures during the shearing process. It is apparent that water plays an important role underground. This research project explores the effect of system and environmental conditions on stiffness and strength properties for artificial discontinuities. Direct shear tests were made on prepared specimens containing a known clay, filling the space between two rock walls under conditions of restricted drainage. Stresses, deformations and water pressures were monitored during the tests.

2. PRINCIPLES INVOLVED - JOINT MECHANICS

a. The Direct Shear Test for Rock Joints

Mathematical modelling of jointed rock masses requires quantitative assessment of the constitutive law for joints. This entails finding every acceptable combination of terms for the vector $\langle u, v, \tau, \sigma \rangle$ where: u and v are the relative shear and normal displacements across the joint; and τ and σ are respectively the shear and normal stress across the joint. One can speak of a

joint constitutive law as $f(u, v, \tau, \sigma) = 0$.

The most direct method of defining the joint constitutive law is to test a specimen representative of the joint surface, and filling material. The sample is oriented in a machine under circumstances wherein the normal and shear stress and displacement, and the environmental conditions are directly controlled or monitored. The direct shear machine is the natural method of achieving this. Direct shear, in fact, is the classical test conducted by workers in friction. For shear through continuous materials such as soils, the triaxial test is considered to provide more uniform stress conditions on the eventual failure plane. However, for rock specimens containing joints oriented in the plane of direct shear, Kutter (1971) showed the direct shear test to be preferable.

b. Parameters of Joint Behavior

The deformability and strength relationships of seams and joints can be described by direct shear testing. The relationship between (τ) and resulting shear displacement (u) developed in the test is expressed in a curve which can be modelled in a physical study or in a digital computer by reporting the changing slopes at different stress levels. The rate of change $(\partial\tau/\partial u)_\sigma$ is called the shear stiffness of the joint. Similarly, the closure of the joint specimen upon application of normal load provides a curve of increasing slope relating normal stress (σ) to normal displacement (v) . The rate of change $(\partial\sigma/\partial v)_\tau$ at any point is the instantaneous normal stiffness. During shearing there is also a tendency for joint thickening (dilation) or closing (contraction), which can be expressed by the rate of change $(\partial\tau/\partial v)_\sigma$. As a result of dilation the volume of the filling material in the sheared zone would tend to change; under conditions of restricted drainage, this tendency would immediately be resisted by the inertia of the water in the sheared zone; the cleft water therefore may suffer an increase or decrease from its original pressure level.

Obviously such a pressure change can be significant in describing the response of the sample to further loading or to the maintenance of existing loads.

It is probable that pore pressure changes are at the core of some stability and support problems both underground and at the surface. Figures 1, 2, and 3, show the form of the constitutive relationship assumed by Goodman and Dubois (1972). The parameters to be evaluated by a test program in addition to the strength parameters and the stiffness terms defined above, are: The maximum closure; normal pressure (σ_T) above which dilatancy cannot occur; and the ratio of residual and peak shear strengths. Of special interest here are the effects of water and water pressure on these joint parameters.

3. PROGRAM PLAN AND VARIABLES

The full range of testing parameters consisted of:

- 2 rock types: granite and sandstone
- 3 roughness ranges for the sandstone and 2 for the granite
- 3 thickness ranges for the filling of the joints
- 2 shear rates (0.1 and 0.28 in./min)
- 4 back pressures (0, 200, 400 and 600 psi)
- 3 normal loads (100, 500 and 1,500 psi)

All combinations of the above parameters represent 532 possibilities. Considering the limitations in time and expenditures of this project, a balanced program of 72 tests was finally selected. Test numbers and parameter values are presented in table 1. Table 2 indicates the total number of tests performed on each rock type and how many of these were used to analyze the influence of the various parameters on the strength and deformability of the joints. This question is taken up again in the discussion of Part IV.

TABLE 1: The Test Program

TEST NO.	ROCK TYPE	JOINT TYPE	ROUGH. (10^{-3} IN)	SHEAR RATE	σ_N (psi)	P_b (psi)	T_i (10^{-2} IN)	$\frac{T_i}{\text{ROUGHN.}}$
1	SANDSTONE	DRY	4.9	$\frac{1}{=0.1}$ in/min	100	-	-	-
2	"	"	45.7	1	1,500	-	-	-
3	"	"	1.9	1	1,500	-	-	-
4	"	"	8.1	1	1,500	-	-	-
5	"	"	1.7	1	1,500	-	-	-
6	"	"	10.4	1	500	-	-	-
7	"	"	27.3	1	500	-	-	-
8	"	"	1.8	1	100	-	-	-
9	"	"	1.5	1	500	-	-	-
10	"	"	4.7	1	500	-	-	-
11	"	"	9.9	1	100	-	-	-
12	"	WET	35.9	1	100	600	-	-
13	"	"	27.5	1	500	600	-	-
14	"	"	12.7	1	100	600	-	-
15	"	"	12.4	1	500	600	-	-
16	"	"	1.1	1	100	600	-	-
17	"	"	2.8	1	500	600	-	-
18	"	"	7.3	1	1,500	600	-	-
19	"	"	6.5	$\frac{1}{2}$	500	200	-	-
20	"	"	7.9		500	200	-	-
21	"	"	35.6	1	1,500	600	-	-
22	"	"	1.8	1	1,500	600	-	-

TABLE 1: The Test Program

TEST NO.	ROCK TYPE	JOINT TYPE	ROUGH. (10^{-3} IN)	SHEAR RATE	σ_N (psi)	P_b (psi)	T_1 (10^{-2} IN)	$\frac{T_1}{\text{ROUGHN.}}$
23	SANDSTONE	WET	14.2	2	1,500	200	-	-
24	"	"	18.0	1	1,000	200	-	-
25	"	FILLED	75.2	1	100	0	8.9	1.18
26	"	"	56.0	1	100	400	7.4	1.32
27	"	"	10.2	1	500	200	1.7	1.66
28	"	"	7.9	1	100	400	1.0	1.26
29	"	"	8.4	2	500	200	0.8	0.10
30	"	"	7.3	2	500	400	0.4	0.055
31	"	"	7.2	1	1,500	200	18.2	25.3
32	"	"	8.0	1	1,500	400	4.5	5.6
33	"	"	17.4	2	1,500	200	3.1	1.78
34	"	"	41.8	1	1,500	400	1.3	0.31
35	"	"	32.1	1	500	0	6.8	2.12
36	"	"	41.1	1	500	400	7.8	1.90
37	"	"	50.7	1	1,500	0	3.7	0.73
38	"	"	9.9	2	1,500	400	0.4	0.40
39	"	"	8.1	1	500	0	2.1	2.52
40	"	"	8.1	1	1,000	0	3.8	4.69
41	"	"	12.6	1	500	200	3.0	2.38
42	"	"	8.9	2	500	200	2.6	2.92
43	"	"	9.8	2	500	400	2.6	2.65
44	"	"	6.6	1	1,500	200	5.2	7.80

TABLE 1: The Test Program

TEST NO.	ROCK TYPE	JOINT TYPE	ROUGH. (10 ⁻³ IN)	SHEAR RATE	σ_N (psi)	P_b (psi)	T_1 (10 ⁻² IN)	$\frac{T_1}{\text{ROUGHN.}}$
45	SANDSTONE	FILLED	6.4	2	1,500	200	4.3	6.72
46	"	"	8.7	2	1,500	400	7.8	8.95
47	"	"	8.2	1	100	0	2.1	2.56
48	GRANITE	DRY	65.5	1	500	-	-	-
49	"	"		1	500	-	-	-
50	"	WET	0.9	1	500	200	-	-
51	"	"	1.9	1	500	600	-	-
52	"	"	67.2	1	500	200	-	-
53	"	"	99.4	1	500	600	-	-
54	"	"	0.9	1	1,500	200	-	-
55	"	"	1.7	1	1,500	600	-	-
56	"	"	76.5	2	500	600	-	-
57	"	"	60.3	1	1,500	600	-	-
58	"	"	56.3	1	1,500	200	-	-
59	"	FILLED	1.1	1	500	200	4.2	38.2
60	"	"	1.1	1	500	600	4.7	42.8
61	"	"	51.6	1	500	200	7.2	1.39
62	"	"	117.5	1	500	400	5.1	0.43
63	"	"	1.4	1	1,500	200	2.9	20.7
64	"	"	2.9	1	1,500	600	4.6	15.9
65	"	"	50.5	2	500	400	4.6	0.91

TABLE 1: The Test Program

TEST NO.	ROCK TYPE	JOINT TYPE	ROUGH. (10 ⁻³ IN)	SHEAR RATE	σ_N (psi)	P_b (psi)	T_1 (10 ⁻² IN)	$\frac{T_1}{\text{ROUGHN.}}$
66	GRANITE	FILLED	66.4	1	500	400	7.3	1.10
67	"	"	66.2	1	1,500	200	2.0	0.31
68	"	"	63.5	1	1,500	400	1.0	0.16
69	"	"	52.5	1	100	400	5.8	1.10
70	"	"	59.4	2	500	400	5.4	0.91
71	"	"	89.4	1	500	0	4.8	0.54
72	"	"	2.3	1	100	400	4.2	18.2

Table 2

Number of Tests on Each Rock Type Used to Analyze
the Influence of the Various Parameters, on the Strength
and Deformability of the Joints

Sandstone: 47 Tests

Granite: 25 Tests

	Normal Load	Roughness	Thickness	Chamber Pressure	Shear Rate
Sandstone					
K_{ss}	47	21	18	29	27
τ_p/τ_r	44	22	22	33	27
u_p	47	23	18	18	18
δ	47	25	22	-	-
Granite					
K_{ss}	20	8	12	16	5
τ_p/τ_r	19	9	10	21	9
u_p	20	8	12	13	8
δ	22	7	15	-	-

K_{ss} : shear stiffness

τ_p/τ_r : ratio of peak shear stress to residual shear stress

u_p : shear displacement at peak stress

δ : dilatation angle

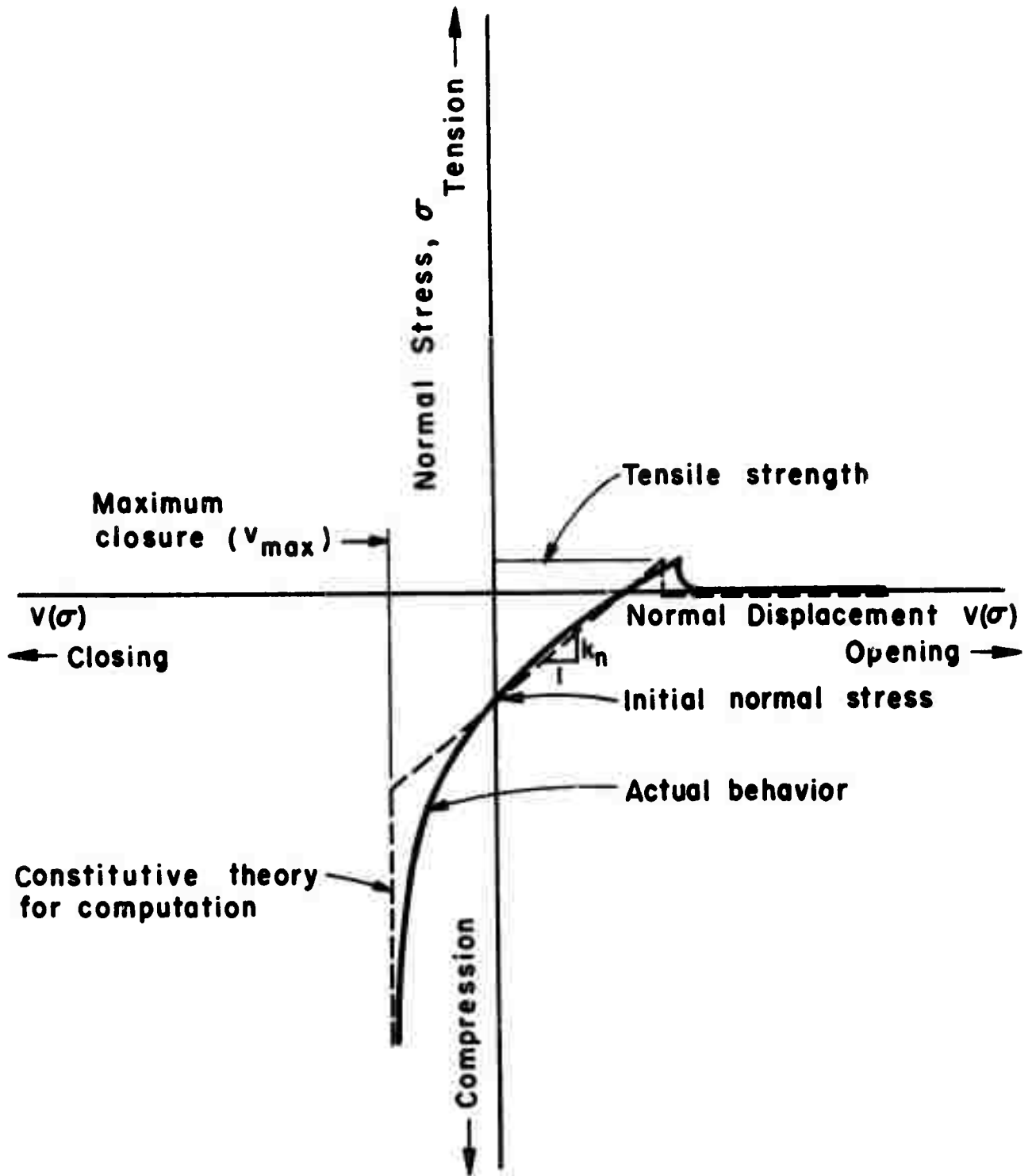


Figure 1. Normal displacement of discontinuity under changing normal stress with constant shear stress

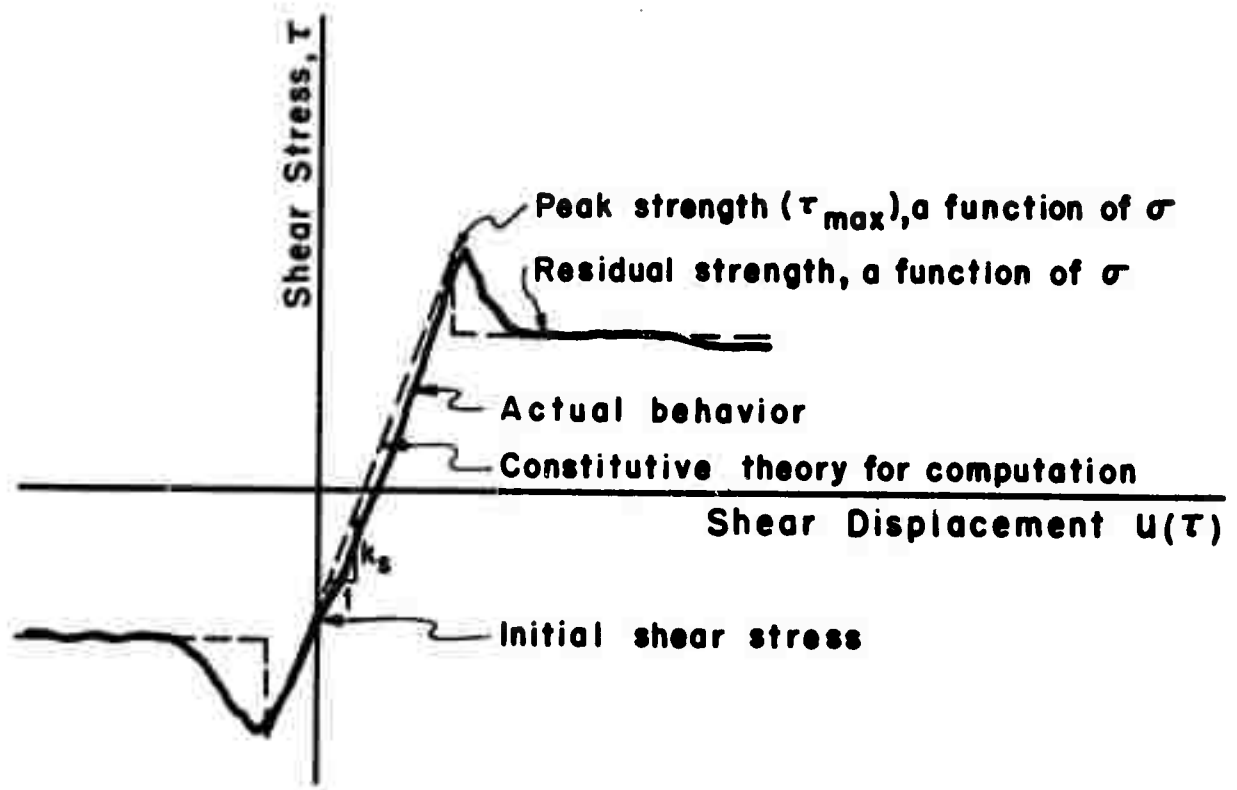


Figure 2. Shear displacement under changing shear stress with constant normal stress

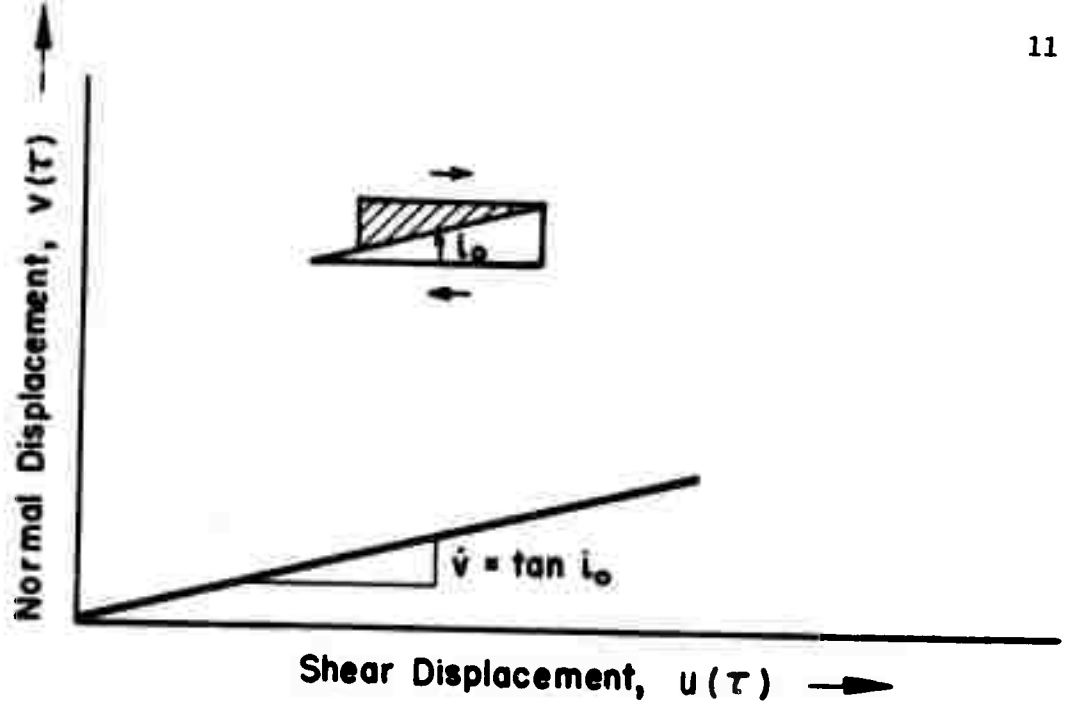


Figure 3a. Initial dilation rate at low normal stress

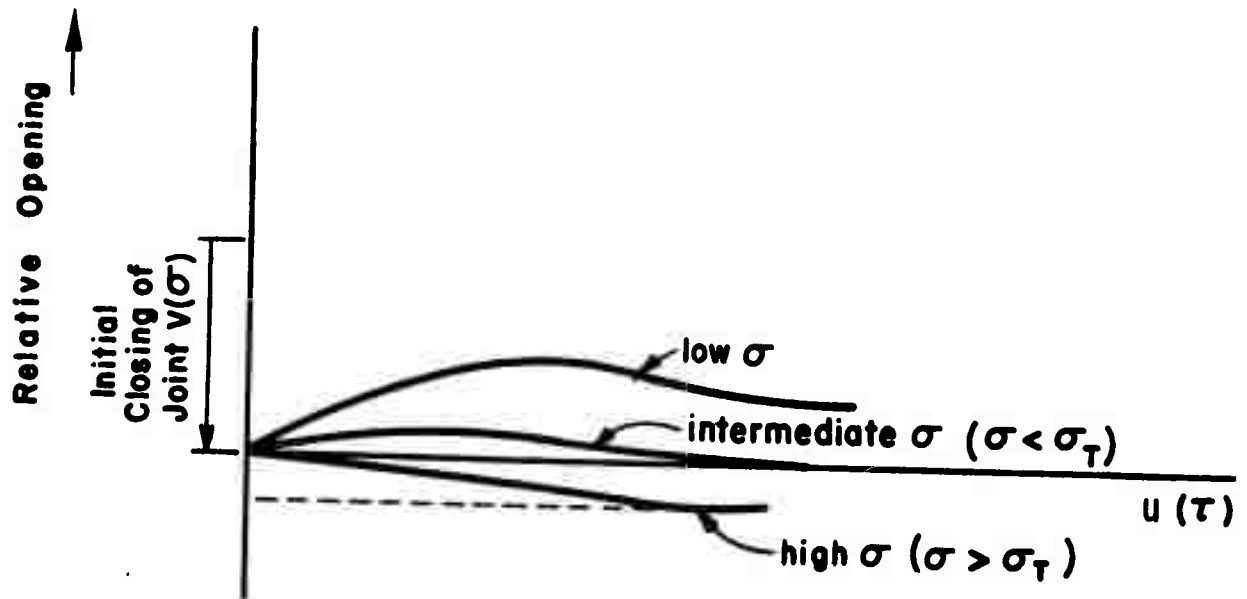


Figure 3b. Actual dilation rates at different normal stresses

PART II: METHOD OF INVESTIGATION

1. EQUIPMENT

The equipment and supplies required for the performance of shear tests include: A large diamond saw for cutting of slabs or prisms (figure 4); a drill and vise assembly for drilling of cores to be tested for index properties (figure 5); a set of shear boxes with appropriate potting compound to set the specimens in their box; a roughness measuring device (figure 6); a direct shear assembly composed of shear machine (figures 7 and 8) and a normal load frame (figure 9); and a data acquisition system (figure 10).

The shear machine can provide shear loads of up to 40,000 lbs. The maximum shear displacement is 3 inches. The sample is contained within a sealed chamber that can sustain an internal water pressure of up to 700 psi; the shear box accommodates samples up to 5 x 5 in. in size. The normal load system is capable of sustaining a load of 40,000 lbs. It was redesigned so that a constant load level can be maintained within $\pm 3/16$ in; this is the maximum normal displacement allowed with the shearing device. The load regulation is achieved by means of an oil/air accumulator of sufficiently large capacity. In practice, piston friction gives a finite stiffness to the normal load system.

Design of a direct shear machine is simple in concept. One provides known loads normal and parallel to the shear plane. Unfortunately rotational tendencies between members of the sample-shear box system cause non uniformities in the stress distribution. As the centroid of the joint contact area moves, the load center should follow it. This can be arranged easily, for example as in the Imperial College shear machine by applying normal loads through a hanging yoke; however, one would then complicate the problem of sealing a water chamber around the specimen. In fact each shear machine represents a compromise of specifications aimed at a particular region of excellence at

the expense of others; e.g. the University of Illinois machine can develop true residual friction values but cannot handle very large specimens and does not have water pressure control in the joint plane; the Berkeley machine was designed for water pressure control, but cannot accommodate large displacements to reach true residual strength for many joint types as the normal load is stationary. Figures 4, 5 and 6 show the shear machine, the controls and the normal loading system. The sample, up to 5-in square, is cemented in a steel box which is under-sheared by two screw driven pistons. The pistons crawl on a track on a rigid support as to prevent vertical movement. Therefore the lower half of the sample can move only horizontally. Vertical movement, but no horizontal movement, is allowed in the upper half of the sample, which carries the water chamber up and down as the joint dilates or contracts. The normal load is supplied by a hydraulic piston. The load is held constant, except for varying piston friction, using an accumulator precharged from a nitrogen bottle to the desired pressure.

The electronic bench is composed of: An amplifier/power supply module made by Kenney Engineering Co., (manufacturer of the direct shear machine); a digital voltmeter and relay matrix (NLS); a 7-channel printer (NLS); and an X-Y-Y' plotter.

The following test variables are monitored by transducers attached to the shear machine: Normal load (σ_n); shear stress (τ); normal displacement (v); shear displacement (u); chamber water pressure (P); and differential water pressures (p_1 or p_2) in the joint. Thus the printer enables recording of all variables simultaneously and the plotter enables monitoring of two variations at a time such as normal and shear stiffness, or pore pressure and dilatancy etc.

2. SPECIMEN PREPARATION

An outline of the testing procedure for direct shear tests is given in

figure 11. The upper half of the diagram represents the steps involved in preparing the specimen.

a. Cutting and Potting

One first cuts a prism of rock 4.75 x 4.75 x 2.75 in. in dimension. Then, depending upon the type of roughness desired for the joint plane the specimen is either

1. sawed in two: roughnesses 1 for granite and sandstone
2. sawed in two and sandblasted: roughness 2 for sandstone
3. split in two: roughness 2 for granite and 3 for sandstone.

It was found that polishing either granite or sandstone would not give a roughness much different from roughness 1. Values of roughness shown in table 1, indicate that this mode of preparation was successful in establishing definite classes of roughness values. The next step consists in potting the sample, as follows (figure 12): The bottom half of the specimen is put into the bottom half shear box and levelled by means of stiff levelling blocks (1). There may or may not be a filler material for the joint. The circumference of the joint surface (3) is protected by a bond breaker (simple masking tape) and the two halves are potted separately by pouring the potting compound (cylcap, primarily sulphur) from holes in the bottom of the boxes, (2) and (4). The bond breaker insures that there will be no sulphur in the shearing plane. Two piezometric holes are then drilled up to the shear plane through guide holes in the bottom half box. These holes will connect, inside the shear chamber, with the water lines and pressure transducers.

b. Roughness and Waviness Measurements

After potting, samples are mounted on the table of the mill shown in figure 6. Micrometers enable precise location of the measuring points. Vertical elevations are obtained by means of a dial gage of sensitivity 10^{-4} in. Eighty-one points are measured on the joint surface (figure 13). The data are

analyzed in terms of roughness and waviness of the surface. The two computer programs used for this analysis were prepared by Mr. Ohnishi and are presented in Appendices B and C with sample outputs. The following information is provided: The mean plane of the observations $z = a_0 + a_1x + a_2y$; an estimate of the standard deviation from the mean plane $\bar{\Delta z}$ -- this is called the roughness of the joint; the maximum positive and negative deviations from the mean plane (peaks and troughs); the average of positive slopes and of negative slopes between points at several distances -- 0.5, 1, 1.5, 2, 2.5, 3, 3.5 and 4 in; the maximum positive and negative slopes for these observations, on the above distances. All slopes are evaluated in the direction of shearing. Values are given in Part III for roughness and waviness.

c. Filling Material

The choice of thickness for the filling material was guided by the roughness measured previously. Three ranges of dimensionless thickness values (T_1/R = initial thickness at beginning of shear/roughness) were obtained for the sandstone and two for the granite; values are presented in Part III.

The filling material first selected was the San Francisco Bay mud. However its composition is quite complex and grain size range is quite large. There was no certainty of obtaining a reproducible joint. Accordingly, a kaolinite clay with controlled properties was finally adopted. It is characterized by the following values (after Houston, 1967):

liquid limit 57%	plastic limit 30%
plasticity index 27%	percent <2 μ = 100%
specific gravity 2.64	activity 0.30

Its expected strength envelope in C-U tests is shown on figure 24).

3. TESTING PROCEDURE

The various steps involved in the performance of a test are described in the lower portion of the diagram on figure 11. With wet tests unfilled or

or with filled joints, the specimens were first saturated, so that developing water pressures would not dissipate in the rock matrix during shear. Filled joints were coated with the kaolinite and their thickness at a normal load equal to that at the beginning of shear was measured in a separate hydraulic press, for maximum accuracy. Each test on filled joints was run in three subtests: 1) application of normal load, and determination of normal stiffness, with continuous plot of u and v vs. σ_n ; 2) application of the back pressure and saturation of the joint plane; 3) shearing -- in this subtest discrete readings were taken of all seven channels σ_n , τ , P , p_1 , p_2 , u and v . In addition continuous plots were obtained on the two x-y-y' plotters: u and v vs. τ on the first one and p_1 and p vs. τ on the second one.

4. PRACTICAL DIFFICULTIES

a. Jacketing of Specimens

Water pressures that would tend to build up during shearing would dissipate by flow away from the joint plane 1) through the wall rock and 2) into the chamber along the edges of the joint. The former can be prevented by using impervious wall rock for the test program; the latter can be prevented by jacketing the specimen. As originally proposed, jacketing would not be incorporated in the test program unless proved necessary as it introduces complexities in specimen preparation, sealing, saturation, and instrumentation. Jacketing is now being done in a continuation of the work, but all tests in the program described here were withunjacketed specimens.

b. Water Pressure Measurement

Since the volume of water in the joint space is small, the stiffness of the water pressure measuring system has an effect on the measurements. Initially, there was too much compressibility in long lines and Bourdon gages. These deficiencies were corrected by moving a differential transducer closer to the specimen. The transducer responds to pressure sources where the

measuring hole intersects the joint plane. This point was not always situated optimally within the joint; in continuation work underway, a distribution network to conduct pressure to the piezometer holes is being evaluated.

c. Filler Material

Ideally, filler material in joints should be natural clay gouge or mylonite of the required thickness preconsolidated to the proper preconsolidation pressure. We do not know what to take as a reasonable value of preconsolidation pressure for a filled shear zone. This is an important parameter. Normally loaded clays can develop induced pore water pressures at peak shear displacement of the order of 40% of the preconsolidation pressure whereas remoulded clays may develop no induced pore pressure at all. Mylonites may be more like remoulded clays than normally consolidated clays.

Attempts to produce shear specimens with normally preconsolidated filling material of predetermined thickness were unsuccessful. Under conditions of only lateral drainage, the required load increment time for consolidation proved large; without multiple consolidometer arrangements the required number of samples therefore could be produced only by accepting considerable delay in the program. Attempts to speed up the consolidation process were frustrated by extrusion of clay from the joint. Instead of preconsolidated filling, therefore, remoulded clay was used. Also, as a substitute for natural gouge, an artificial kaolinite was selected for filling so that uniformity and homogeneity could be insured. However as kaolinite is representative of some faults and seams and no single clay gouge material can be representative of all faults and seams, the use of kaolinite for filler is appropriate.

d. Normal Stiffness Measurements

To measure the normal stiffness of the joint, one must subtract the

shortening of the sample without a joint from that of the sample with a joint. Since the measurement utilizes the difference of large numbers, errors can be large unless care is taken to insure that the samples and procedures are in all respects the same except for the existence of the joint. Because of the many faceted nature of the experimental program, it was not convenient to meet this restraint in all tests, and therefore the program did not generally yield good results for normal stiffness values.

Reproduced from
best available copy.

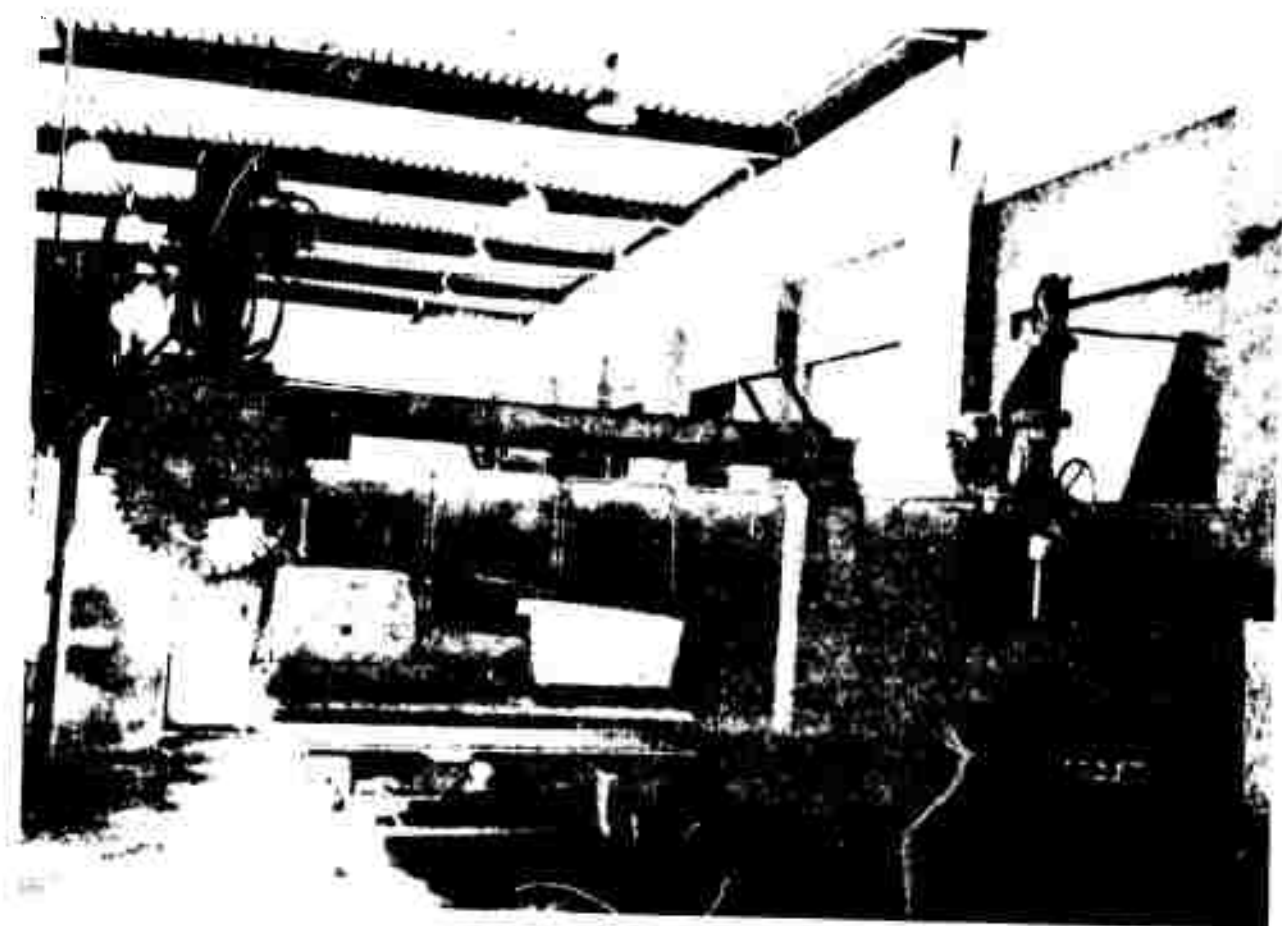


FIGURE 4 : 36-INCH SAW ASSEMBLY

Reproduced from
best available copy.

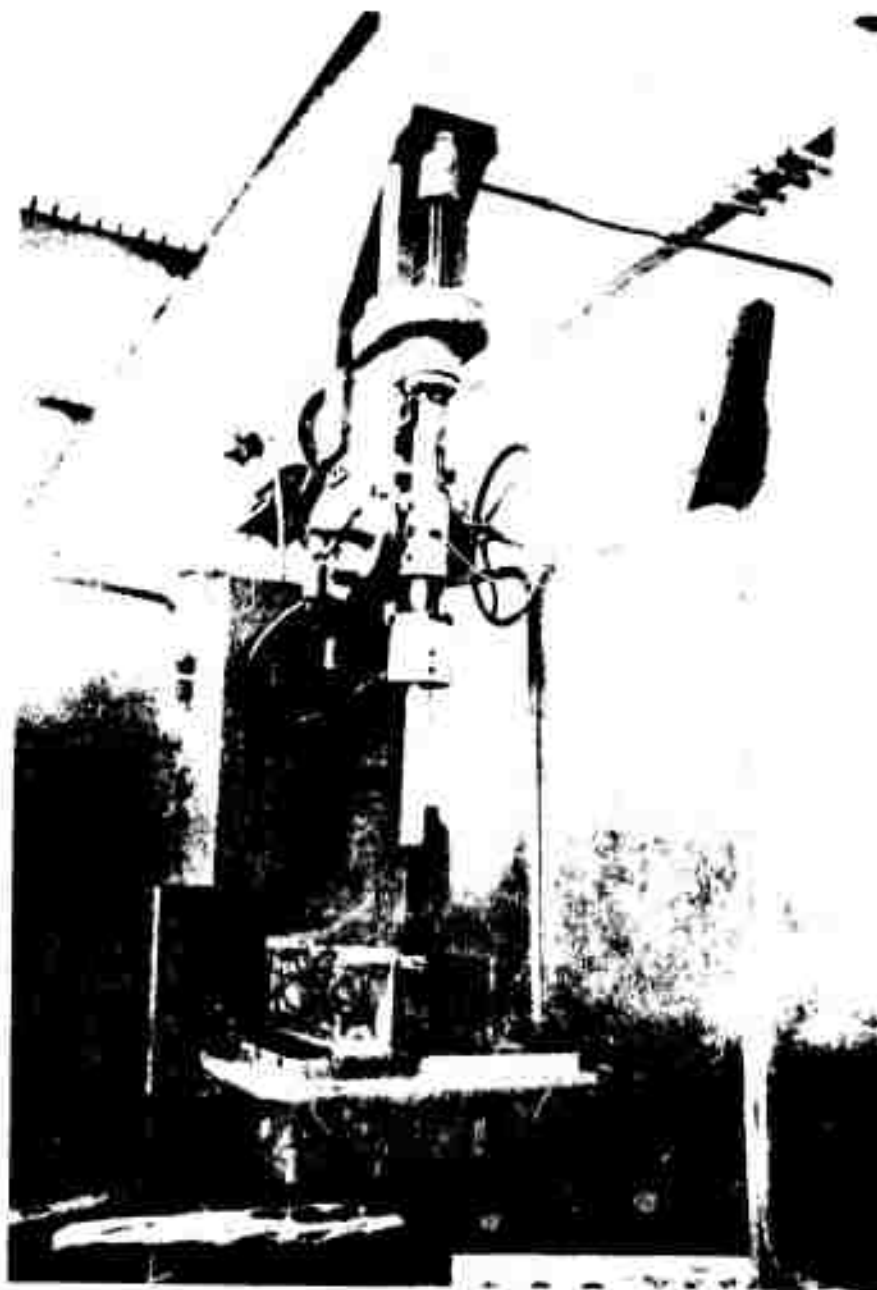


FIGURE 5 : DRILL AND VISE ASSEMBLY

Reproduced from
best available copy.

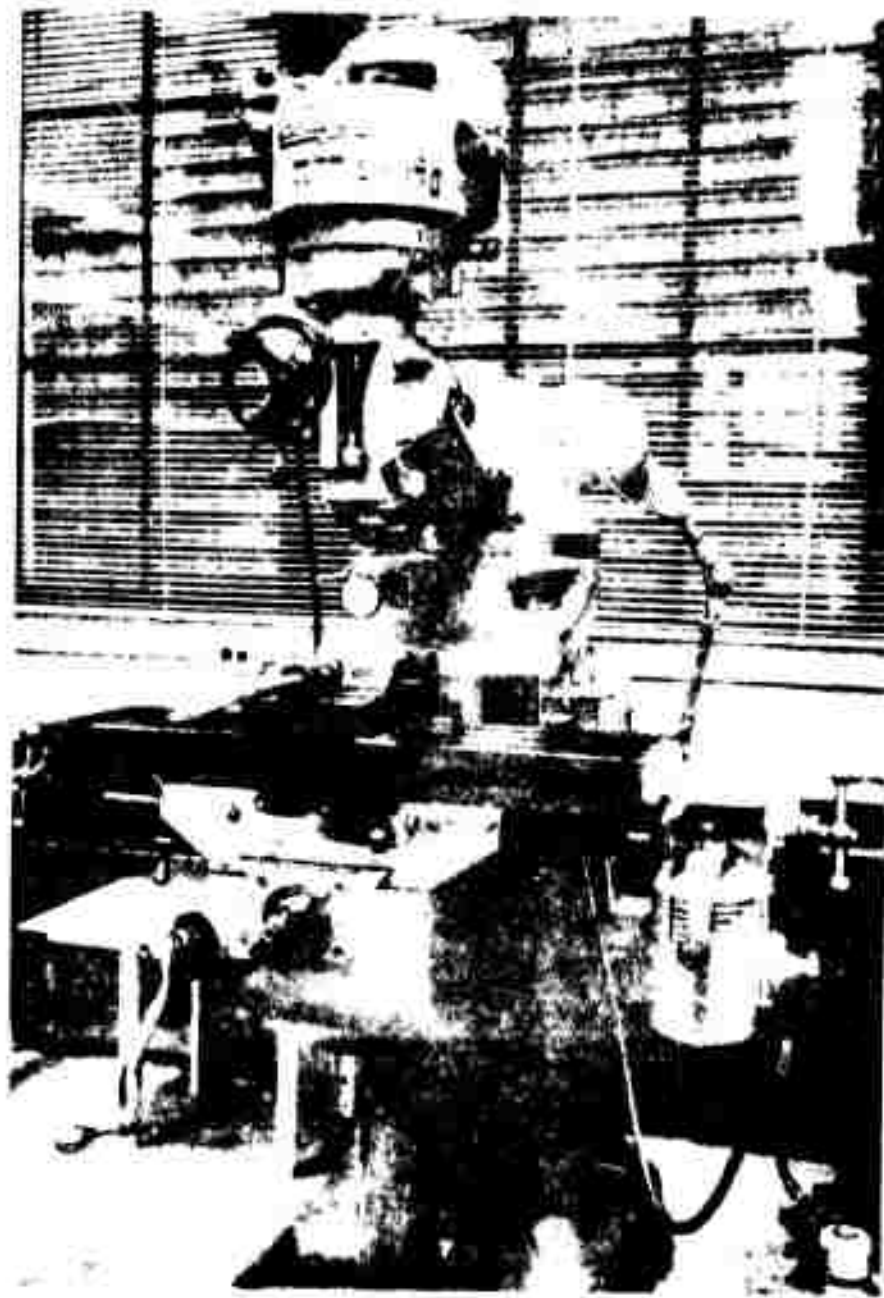


FIGURE 6: ROUGHNESS MEASURING SYSTEM ON MILL TABLE

Reproduced from
best available copy.

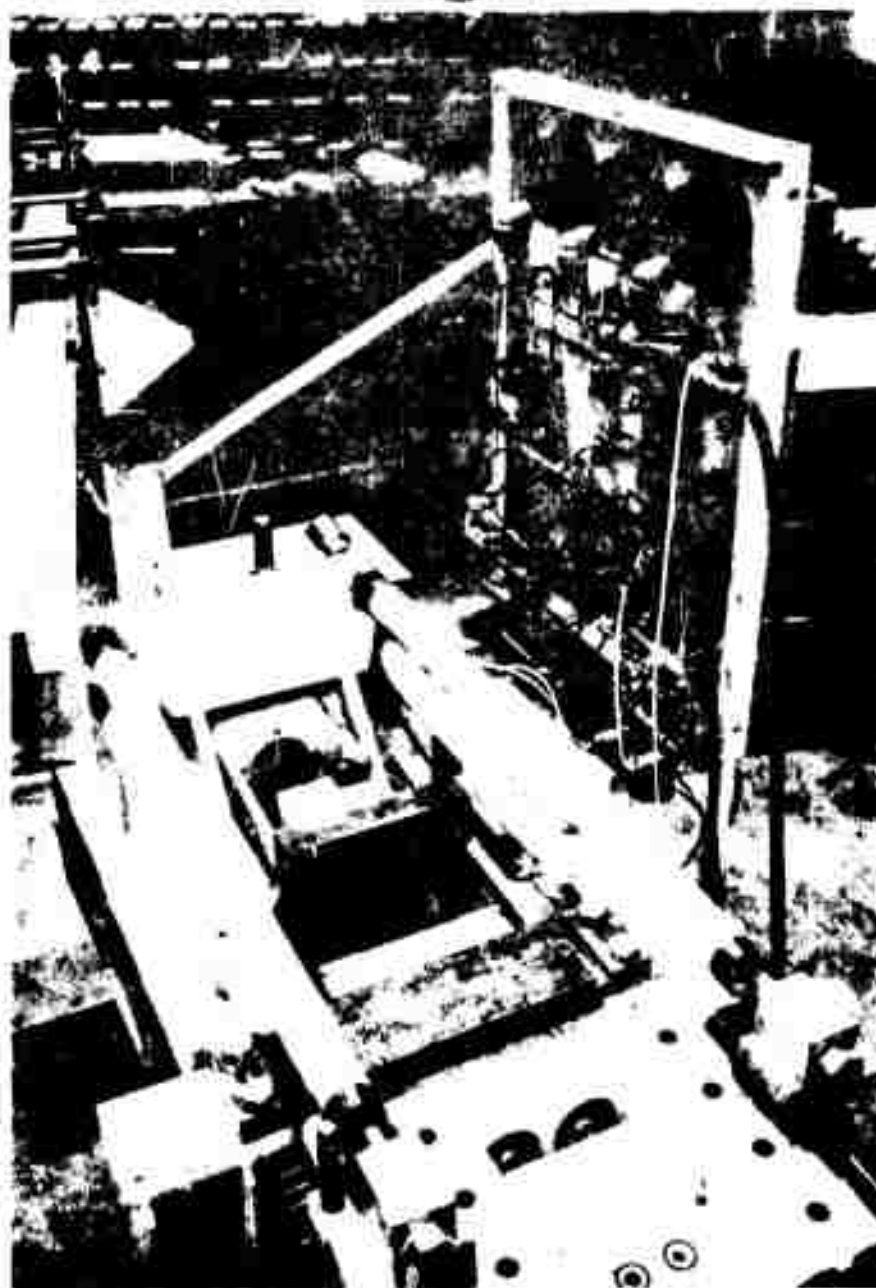


FIGURE 7 : DIRECT SHEAR MACHINE , TOP REMOVED

Reproduced from
best available copy.

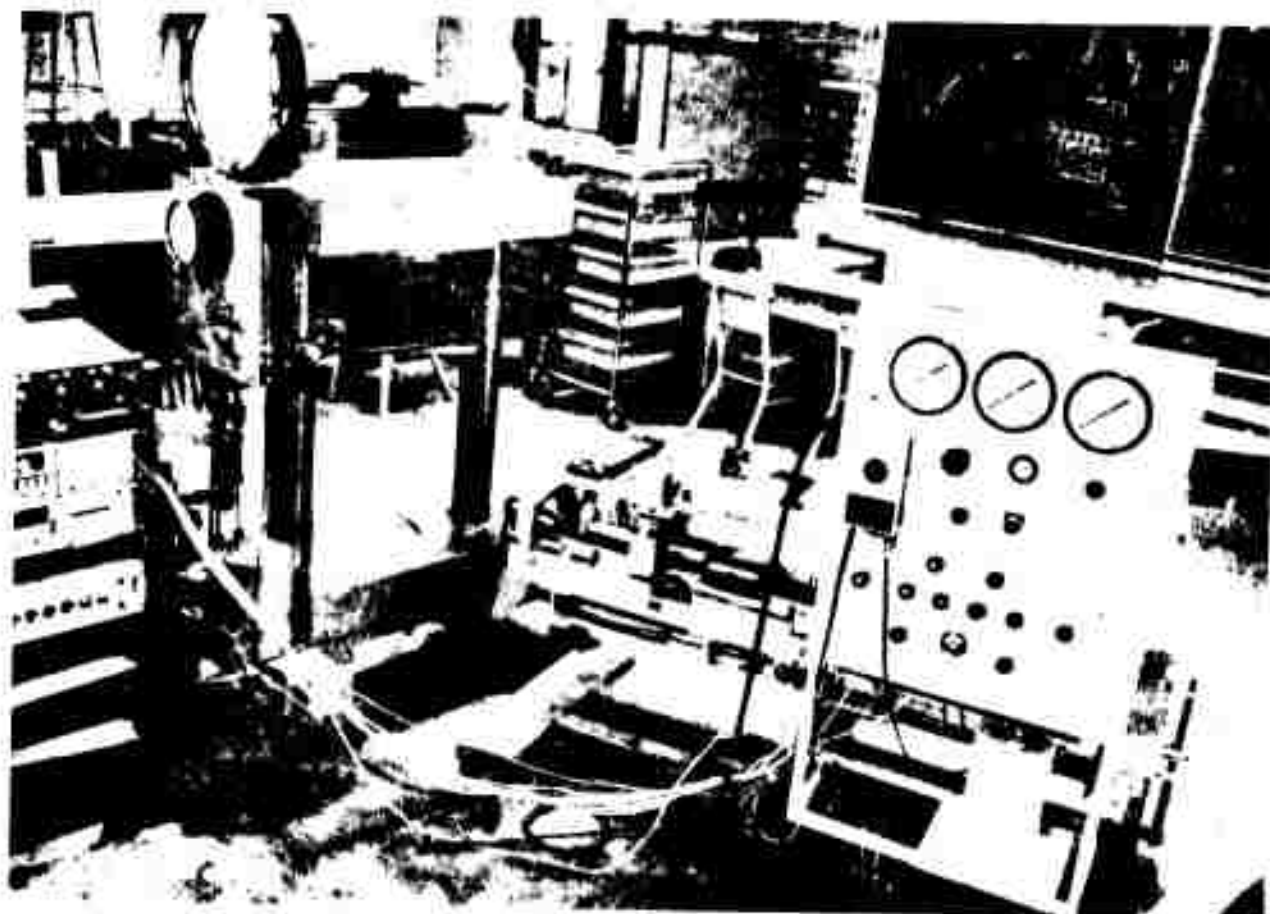


FIGURE 8 : SHEAR TESTING ASSEMBLY AND CONTROLS

Reproduced from
best available copy.

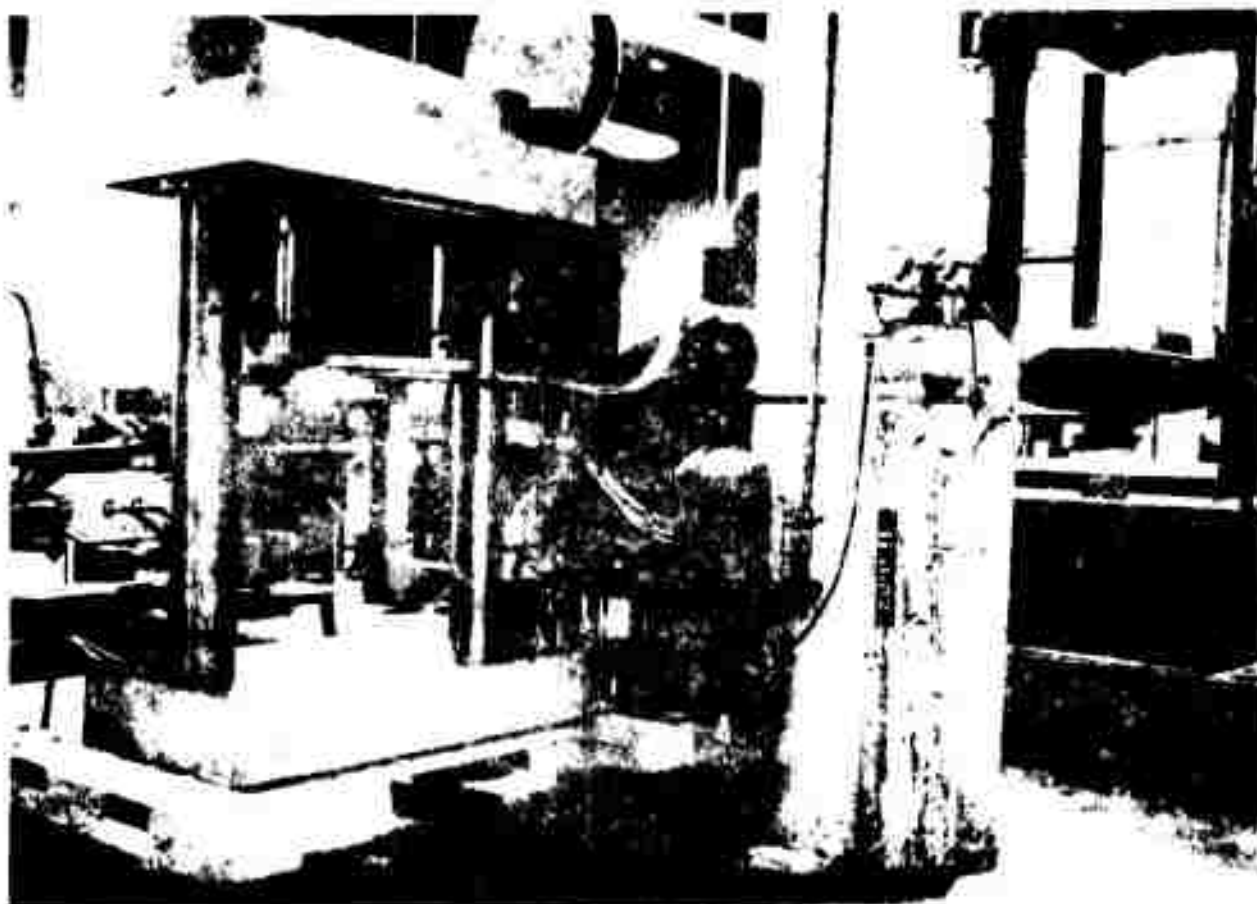


FIGURE 9 : NORMAL LOADING DEVICE AND REGULATOR SYSTEM

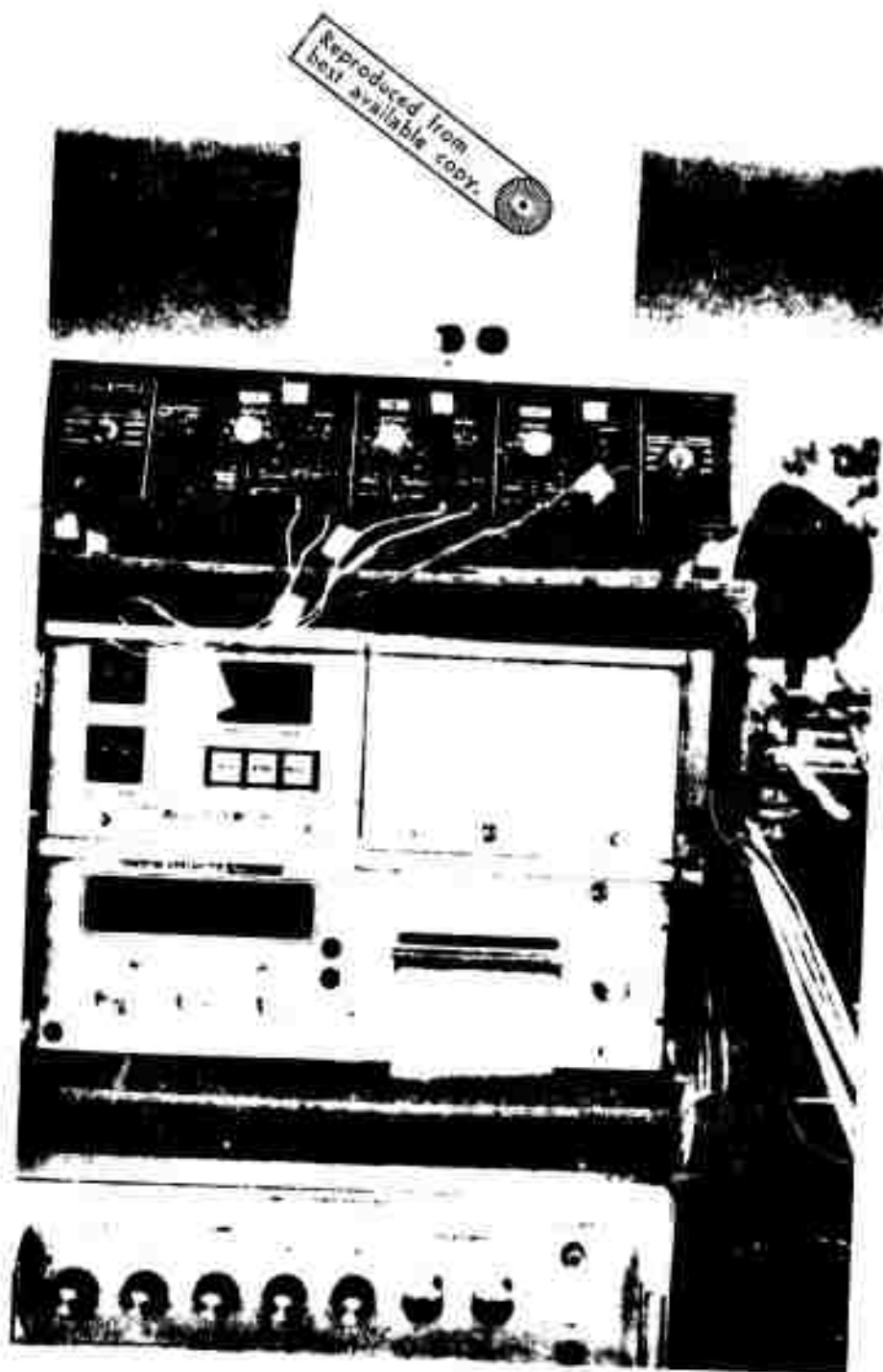
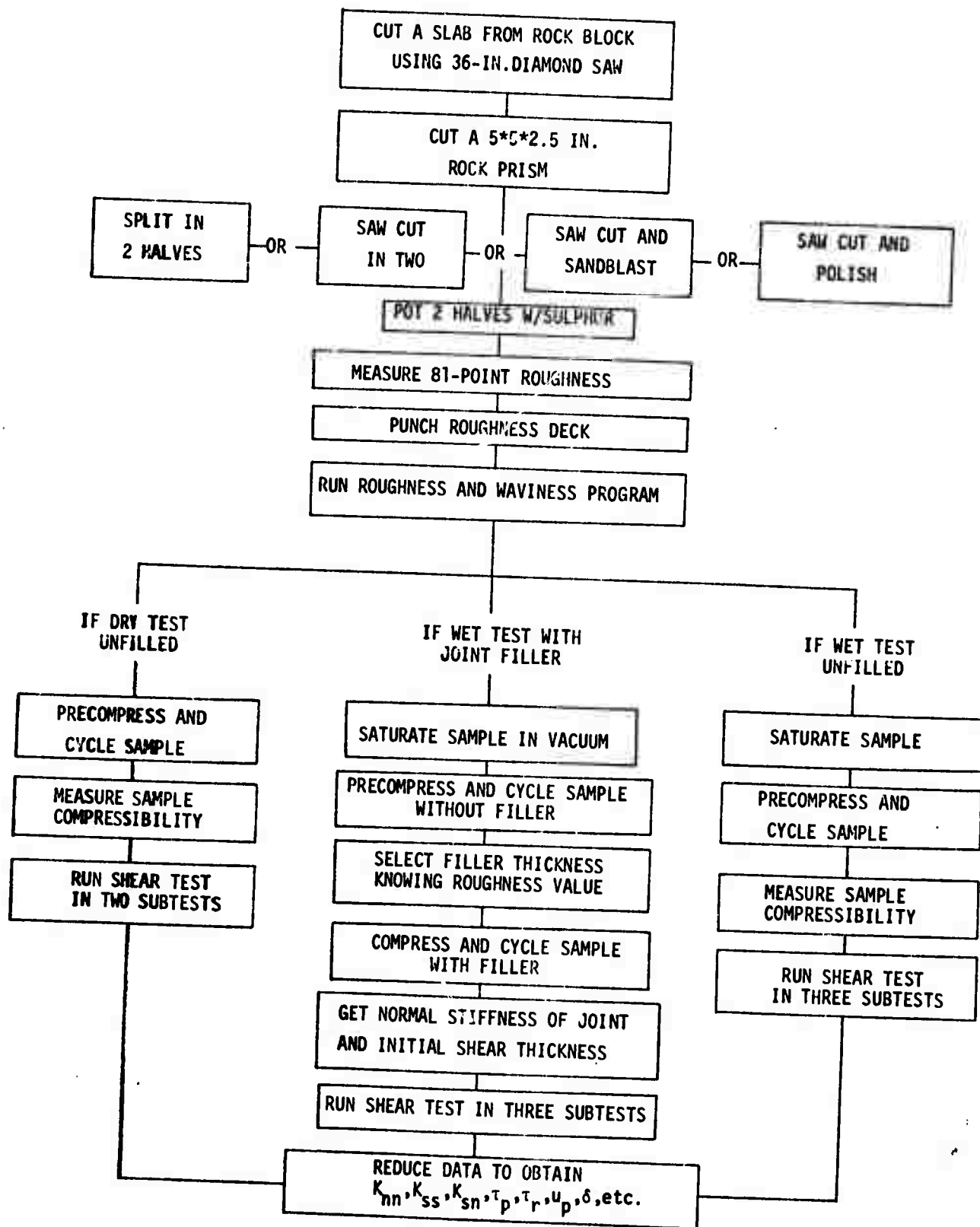


FIGURE 10: ELECTRONIC DATA RECORDING SYSTEM



OUTLINE OF TESTING PROCEDURE FOR DIRECT SHEAR TESTS

FIGURE 11

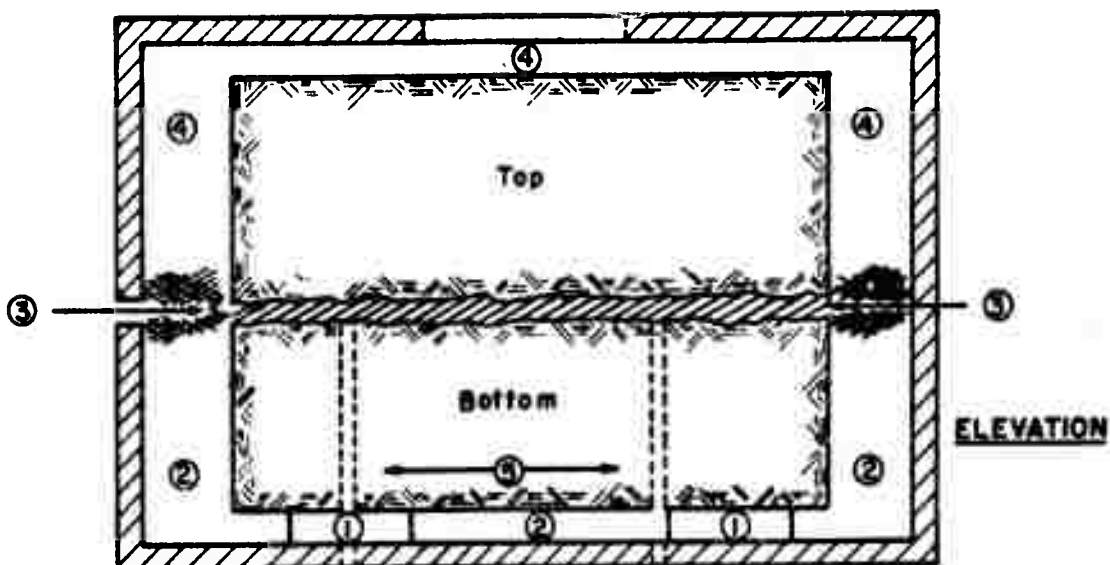


FIGURE 12: SHEAR SPECIMEN ASSEMBLED FOR TESTING (LEGEND IN TEXT)

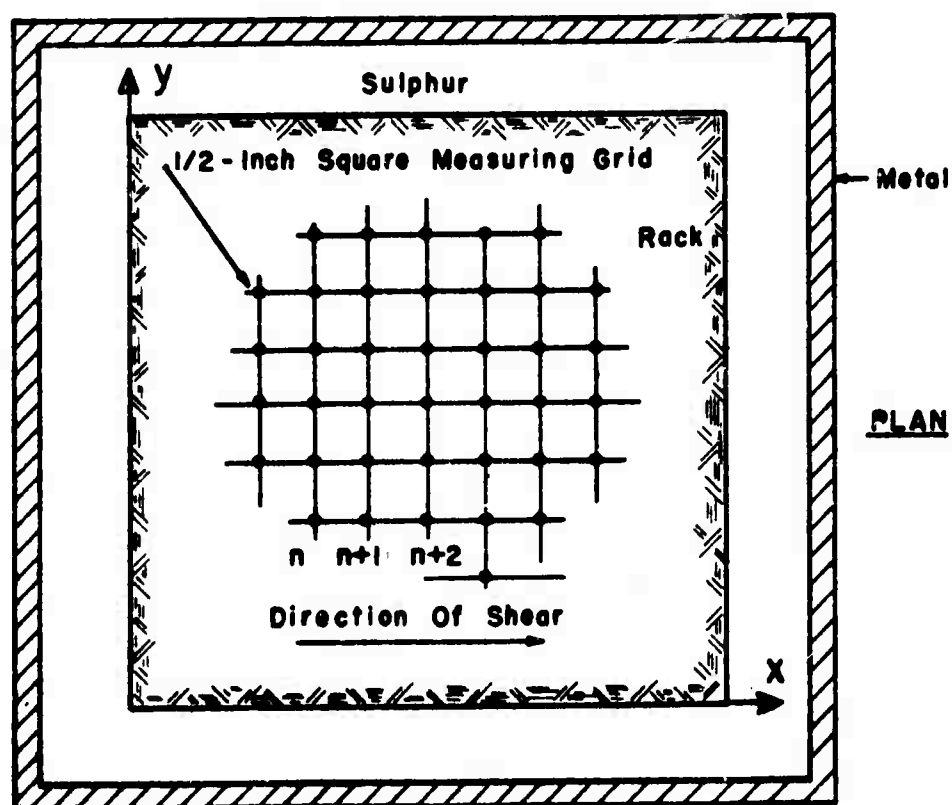


FIGURE 13: HALF SPECIMEN LAY-OUT FOR ROUGHNESS MEASUREMENT

PART III: RESULTS OF THE TEST PROGRAM

1. PROPERTIES OF THE "GRANITE" AND THE SANDSTONE

a. Petrographic Examination

The rocks selected consist of a fine grained friable quartz arenite, and a porphyritic biotite, hornblende quartz diorite. They are described in Appendix A (prepared by Mr. Quentin Gorton).

b. Strength-Deformability and Bulk Properties

Index tests were conducted and their results are presented in table 3.

2. ROUGHNESS AND WAVINESS OF THE JOINT PLANES

a. Roughness

The values of joint roughness were presented in table 1 and are re-grouped in figures 14 and 15 where it can be seen that the various modes of preparation established distinct classes of roughness.

b. Waviness

The average slope angle is compared to the length of observation in figure 16 for various roughnesses. There is a sharp decrease in slope angle where going from 0.5 inch to a few inches. This may well indicate that at the scale of field observation the average slope angle is no more than 1 degree. Figure 17 indicates the physical relationship between measured roughness and the maximum positive slope angle. Such a relationship can probably not be applied directly to field situations considering the great difficulty in accurately describing in-situ the two parameters involved.

3. THICKNESS OF JOINT FILLER

Values for dimensionless thickness of the joint filler were presented in table 1 and are reproduced in figures 18 and 19. Without sedimentation of the clay material, it proved difficult to establish precise thickness, set

in advance. However, the measurements shown in figures 18 and 19 indicate that as for roughness, definite classes of thicknesses were established for both rock types. In this context one must remember that a value of $T_1/R < 1$ means that the asperities of the filled joint do interlock whereas for greater values of T_1/R there is a tendency to shear through the filling material.

4. DEFORMABILITY AND STRENGTH DATA

The deformability and strength values for tests on sandstone and granite joints dry and wet, filled and unfilled are presented in table 4. The order of presentation of the tests which are numbered from 1 to 72 is: sandstone dry (11), wet (13), filled (23), and granite dry (2), wet (9) and filled (14).

The following were directly measured or computed for all tests:

- peak normal stress σ_p maintained as close as possible to the initial normal stress value
- peak shear stress, τ_p
- ratio τ_p/σ_p
- residual shear stress τ_r
- shear displacement at peak, u_p
- normal displacement at peak, v_p
- dilatancy angle at peak $\delta = \text{Arctan}(u_p/v_p)$; this angle is positive (dilation) or negative (contraction)
- shear stiffness, K_{ss} computed from the linear portion of the (τ, u) curve.

The dilation or contraction of the joint at peak (P) and beyond is illustrated in the last column by wide or narrow signs depending upon the relative amount of dilation (\nearrow) or contraction (\searrow). The normal stiffness is given below for a few selected tests, following the discussion of Part II, paragraph 4 d.

Concerning values of the shear stiffness (K_{ss}), the following must be remembered here:

1. The shear stiffness is defined as peak shear stress, to peak shear displacement ratio,

2. Accordingly a high K_{ss} can correspond to a high peak strength or a low peak displacement. So, both a strong joint with interlocking asperities, and a weak joint with very thick filler which very quickly attains its residual strength, can have high shear stiffness before their peak.

Table 5
Normal Stiffness Values for Selected Tests on Filled Joints

Test No.	Rock Type	K_{nn} (10^4 psi/in)	K_{ss} (10^4 psi/in)	K_{nn}/K_{ss}	T_1/R	Dilatancy (°)
25	Sandstone	2.06	0.10	20.6	1.18	+ 7.5
26	"	1.99	0.71	2.8	1.32	+10.0
28	"	1.99	0.47	4.2	1.26	0
47		2.00	0.61	3.3	2.56	+ 1.8
69	Granite	1.92	0.09	22.6	1.10	+ 2.6
70	"	6.23	0.28	22.3	0.91	+ 5.5
71	"	24.9	0.30	83.0	0.54	+ 3.7
72	"	2.66	1.50	1.4	18.2	0

5. WATER PRESSURE DATA

The results of tests with non zero differential water pressures ($P - p_1$ or $P - p_2 = \Delta$), are presented in table 6 together with other relevant data from the tests. When discrete readings were taken during the tests, they are all given. It can be noted that both positive and negative values of the transient pore pressures were observed.

All results presented above are now discussed in Part IV.
A typical test record is given in Appendix D (Test #61).

Table 3

Summary of Index Properties for the Rock Types of the Shear Program*

	"Sierra White" Granite (Porphyritic Quartz Diorite)	Lyon's Sandstone (Fine Grained Quartz Sandstone)
Mineralogy	quartz 25% biotite 5% plagioclase 55% muscovite 4% K-feldspar 8% hornblende 3%	quartz 99% calcite (trace) hematite 1%
Grain size	1 to 3 mm	0.1 to 0.2 mm
Unconf. comp. strength dry sat	13600 psi 11100 psi	4260 psi 4260 psi
E at 50% strength dry sat	3.6×10^6 psi 3.2×10^6 psi	0.60×10^6 psi 0.36×10^6 psi
ν at 50% strength dry sat	0.25 -	0.30 0.26
Tensile strength (dry)	660 psi 545 psi	260 psi 135 psi
Modulus of Rupture (dry)	2860 psi	520 psi (fracture // to bedding)
Cohesion (dry)	2200 psi	550 psi
Initial friction angle (dry)	54°	56°
Residual friction angle(dry)	48°	33°
Porosity	4.6%	11%
Permeability (Rw)	not measurable	3.3 millidarcys

* Mechanical properties of the sandstone given on cores perpendicular to the bedding.

Table 4
Strength and Deformability Data for Tests of the Shear Program

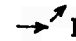
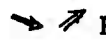
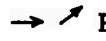

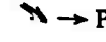











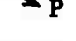










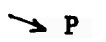
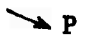

Test No.	σ_p (psi)	τ_p (psi)	$\frac{\tau_p}{\sigma_p}$	τ_r (psi)	$\frac{\tau_p}{\tau_r}$	u_p (10^{-2} in)	δ degrees	K_{ss} (10^4 psi/in)	Dilation at Peak
1	135	35	0.26	35	1.00	2.8	+ 2.5	0.13	 P
2	1,530	1,650	1.07	1,150	1.43	20.4	+ 0.6	0.81	 P
3	1,490	1,010	0.68	990	1.02	12.0	+ 0.4	0.84	 P
4	1,490	760	0.51	760	1.00	13.0	- 2.2	0.58	 P
5	1,500	1,000	0.67	890	1.12	11.4	- 1.6	0.88	 P
6	450	230	0.51	208	1.10	20.0	- 5.5	0.12	 P
7	500	470	0.94	440	1.07	9.6	- 0.4	0.46	 P
8	85	10	0.12	8	1.25	3.0	0	0.03	 P
9	465	230	0.50	230	1.00	5.6	0	0.45	 P
10	480	280	0.58	260	1.08	6.6	0	0.42	 P
11	108	24	0.22	24	1.00	10.0	- 3.9	0.02	 P
12	228	218	0.95	218	1.00	20.0	+ 4.4	0.14	 P
13	600	580	0.97	520	1.12	14.4	+ 0.9	0.40	 P
14	102	70	0.69	70	1.00	2.0	- 4.8	0.35	 P
15	480	420	0.88	420	1.00	14.0	- 0.2	0.30	 P
16	98	25	0.26	25	1.00	2.0	0	0.13	 P
17	500	560	1.12	545	1.02	14.0	- 1.4	0.40	 P
18	1,520	1,005	0.66	980	1.02	19.0	- 0.1	0.53	 P
19	450	275	0.61	275	1.00	16.0	- 0.4	0.17	 P
20	460	285	0.62	285	1.00	10.0	- 1.0	0.29	 P
21	1,500	1,210	0.81	975	1.24	11.0	- 0.6	1.10	 P
22	1,350	1,115	0.82	1,005	1.10	13.0	+ 0.8	0.77	 P
23	1,500	1,015	0.68	1,015	1.00	16.8	- 1.7	0.60	 P
24	1,120	710	0.63	710	1.00	16.0	- 2.0	0.44	 P
25	100	145	1.45	145	1.00	14.0	+ 7.5	0.10	 P
26	100	71	0.71	71	1.00	1.0	+ 10.0	0.71	 P
27	500	220	0.44	183	1.20	2.0	- 3.2	1.10	 P
28	100	28	0.28	23	1.22	0.6	0	0.47	 P
29	500	192	0.38	69	1.13	3.7	- 1.7	0.52	 P
30	500	261	0.52	224	1.16	2.5	- 1.2	1.04	 P

Table 4 (continued)

Test No.	σ_p (psi)	τ_p (psi)	$\frac{\tau_p}{\sigma_p}$	τ_r (psi)	$\frac{\tau_p}{\tau_r}$	u_p (10^{-2} in)	δ degrees	K_{ss} (10^4 psi/in)	Dilation at Peak
31	1,600	310	0.19	255	1.21	10.6	- 2.5	0.24	→ P
32	1,310	460	0.35	375	1.22	4.5	0	1.02	→ P
33	1,510	510	0.34	485	1.05	6.6	- 0.7	0.77	→ P
34	1,500	735	0.49	695	0.49	10.9	- 0.6	0.67	→ P
35	500	175	0.35	155	0.35	2.8	- 1.2	0.62	→ P
36	500	185	0.37	170	0.37	3.7	- 1.8	0.50	→ P
37	1,440	620	0.43	620	0.43	5.4	- 0.6	1.15	→ P
38	1,420	440	0.31	410	1.07	10.0	- 2.0	0.44	→ P
39	485	120	0.25	75	1.60	2.0	0	0.60	→ P
40	860	310	0.36	240	1.29	6.5	+ 0.5	0.48	→ P
41	500	188	0.38	157	1.19	2.4	- 3.4	0.78	→ P
42	535	185	0.35	155	1.19	2.7	- 2.3	0.68	→ P
43	500	158	0.32	100	1.58	4.5	- 0.4	0.35	→ P
44	1,460	465	0.32	405	1.15	9.6	- 0.5	0.49	→ P
45	1,430	460	0.32	400	1.15	6.6	- 1.0	0.70	→ P
46	1,400	430	0.31	385	1.12	9.5	- 0.6	0.45	→ P
47	100	98	0.98	57	1.70	1.6	+ 1.8	0.61	→ P
48	500	1,660	3.32	690	2.40	11.2	+ 11.1	1.48	→ P
49	500	1,163	2.32	665	1.75	9.0	- 1.8	1.83	→ P
50	540	420	0.78	420	1.00	-	-	-	→ P
51	500	320	0.64	320	1.00	16.0	- 0.6	0.20	→ P
52	640	660	1.03	505	1.30	18.0	+ 1.1	0.28	→ P
53	475	830	1.75	670	1.24	16.0	+ 4.0	0.52	→ P
54	1,570	1,100	0.77	1,100	1.00	25.0	- 0.6	0.44	P
55	1,470	975	0.66	975	1.00	20.0	- 0.2	0.49	→ P
56	485	670	1.38	575	1.17	10.6	+ 7.1	0.63	→ P
57	1,380	1,500	1.09	922	1.63	8.8	-	1.71	→ P
58	1,000	885	0.89	822	1.08	19.0	+ 4.0	0.47	→ P
59	505	255	0.51	255	1.00	1.4	- 14.0	1.82	→ P
60	495	140	0.28	140	1.00	0.8	- 45.0	1.75	→ P
61	620	540	0.87	450	1.20	10.4	- 0.6	0.52	→ P
62	510	480	0.94	365	1.31	5.0	+ 12.8	0.96	→ P
63	1,470	340	0.23	340	1.00	2.4	- 1.2	1.51	→ P

Table 4 (Continued)


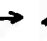

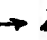










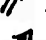



Test No.	σ_p (psi)	τ_p (psi)	$\frac{\tau_p}{\sigma_p}$	τ_r (psi)	$\frac{\tau_p}{\tau_r}$	u_p (10^{-2} in)	δ degrees	K_{ss} (10^4 psi/in)	Dilation in Peak
64	1,480	365	0.25	290	1.26	14.6	- 3.2	0.25	 P
65	624	385	0.62	346	1.11	20.0	+ 1.6	0.19	  P
66	500	510	1.02	450	1.13	14.8	+ 4.2	0.34	  P
67	1,440	1,345	0.93	1,170	1.15	7.2	- 0.9	1.87	  P 
68	1,500	650	0.43	602	1.07	24.0	- 3.5	0.27	   P
69	100	120	1.20	120	1.00	13.6	+ 2.6	0.09	 P 
70	510	550	1.08	485	1.13	19.0	+ 5.5	0.28	  P
71	500	502	1.00	395	1.27	16.8	+ 3.7	0.30	  P
72	100	57	0.57	53	1.07	0.3	0	1.50	 P

Table 6

Water Pressures Observed for Tests
on Sandstone and Granite Joints

Test No.	ΔU Observed (psi)	Back Pressure (psi)	Roughness (10^{-3} in)	Shear Rate	T_1/R
19	-0.25	200	6.5	1	0
22	-4.0	600	1.8	1	0
24	-2.7	200	18.0	1	0
25	+0.3	0	75.2	1	1.2
	+0.3				
	+0.3				
26	-0.2	400	56.0	1	1.32
27	+1.6	200	10.2	1	1.66
	+1.0				
28	-0.1				
	-0.1	400	7.9	1	1.3
29	+5.0	200	8.4	2	0.10
	+5.0				
30	-3.1	400	7.3	2	0.05
	-3.7				
32	-0.8	400	7.9	1	5.6
33	+5.5	200	17.4	2	1.8
34	+4.9	400	41.8	1	0.31
35	-1.7	0	32.1	1	2.12
36	+9.9	400	41.1	1	1.90
37	-1.2	0	50.7	1	0.73
38	+0.9	400	9.9	2	0.4
39	-0.5	0	8.1	1	2.5
40	-0.5	0	8.1	1	4.7
41	+0.3	200	12.6	1	2.4
	+0.4				
42	-0.3	200	8.9	2	2.9
43	+3.2	400	9.8	2	2.7
44	-0.2	200	6.6	1	7.8
46	+0.8	400	8.7	2	8.9

Table 6 (continued)

Test No.	ΔU Observed (psi)	Back Pressure (psi)	Roughness (10 ⁻³ in)	Shear Rate	T_1/R
47	-1.1	0	8.2	1	2.6
51	-0.25	600	1.9	1	0
52	-0.20	200	67.2	1	0
54	+2.8	200	0.9	1	0
60	+0.7	600	1.1	1	42.8
	-1.4				
61	+25.2	200	51.6	1	1.4
	+22.6				
62	+0.6	400	117.5	1	0.43
	-5.7				
	+0.7				
	+0.6				
	+7.3				
65	-0.1	400	50.5	2	0.91
	-0.3				
	-0.2				
66	+0.2	400	66.4	1	1.10
	-0.3				
67	+1.8	200	66.2	1	0.31
68	+7.5	400	63.5	1	0.36
69	+0.6	400	52.5	1	1.10
	+1.4				
	+2.2				
70	+2.6	400	59.4	2	0.91
71	+5.4				
	-0.3	0	59.4	1	0.54
72	+0.4	400	2.3	1	18.2
	-0.1				

Table 7
Influence of the Test Program Variables
on Joint Deformability Parameters

Variation $\partial X/\partial Y$: Sandstone

X	Y				
	σ_n	R	T_1/R	t	P_b
K_{ss}	dry, wet: >0 filled : ?	dry, wet >0 for $R > 25$	>0 ? for $T_1/R > 10$	slightly <0	wet tests: >0 filled : ?
u_p	>0	dry: slightly >0 wet: ≈ 0 except >0 for $\sigma_n < 100$	≈ 0	slightly >0?	slightly >0?
δ	<0 counteract each other	>0	≈ 0 $T_1/R < 20$ slightly >0 for $T_1/R > 20$	-	-

Variation $\partial X/\partial Y$: Granite

X	Y				
	σ_n	R	T_1/R	t	P_b
K_{ss}	wet >0	>0 when $R \geq 70 \times 10^{-3}$	>0	inconclusive	wet : >0 filled: ≈ 0
u_p	>0	Apparently <0	inconclu- sive	inconclusive	apparently <0
δ	wet: >0? at $\sigma_n < 1,500$ filled: <0	>0	-	-	-

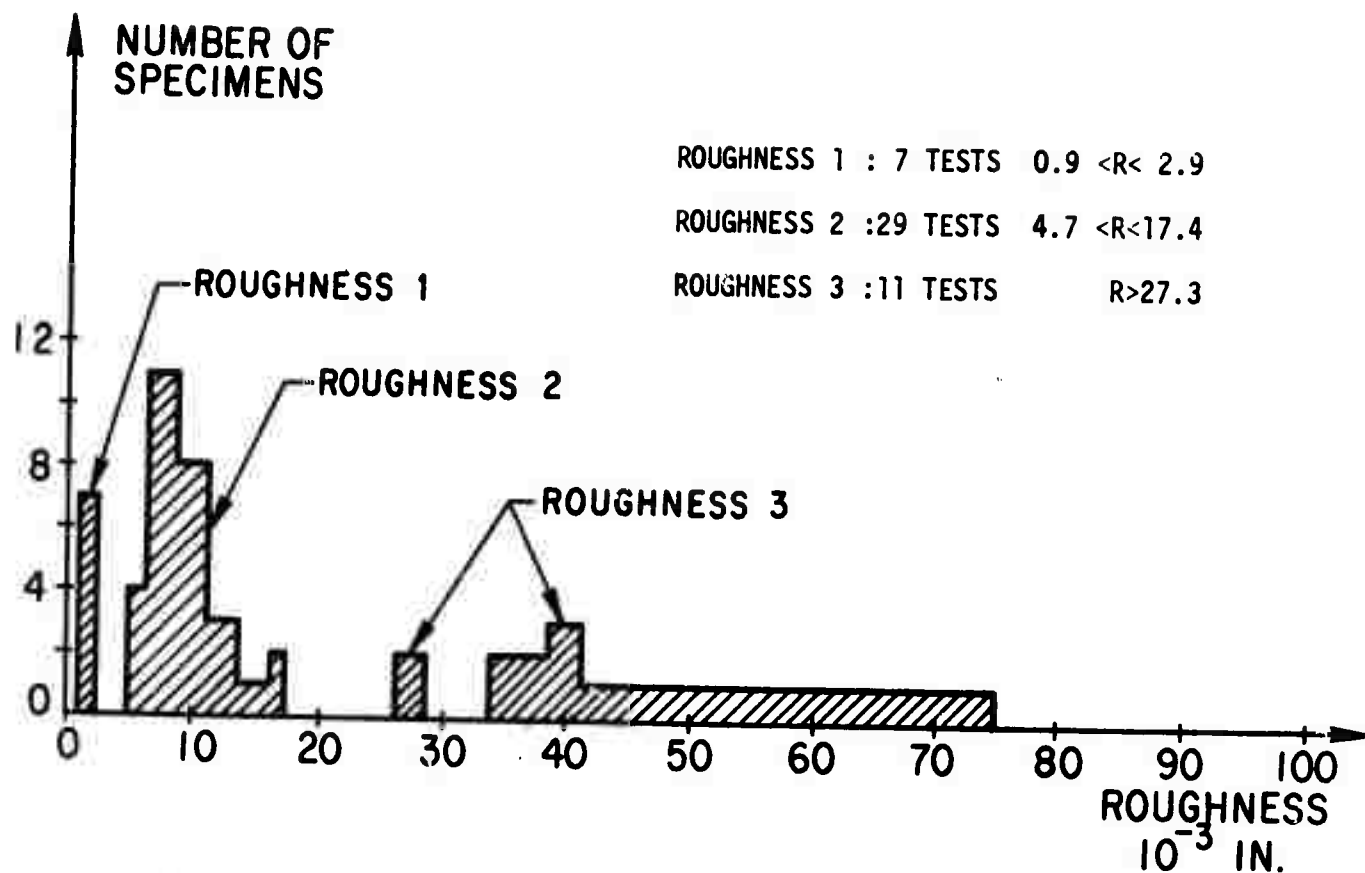


FIGURE 14 : ROUGHNESS DISTRIBUTION OF SANDSTONE JOINTS

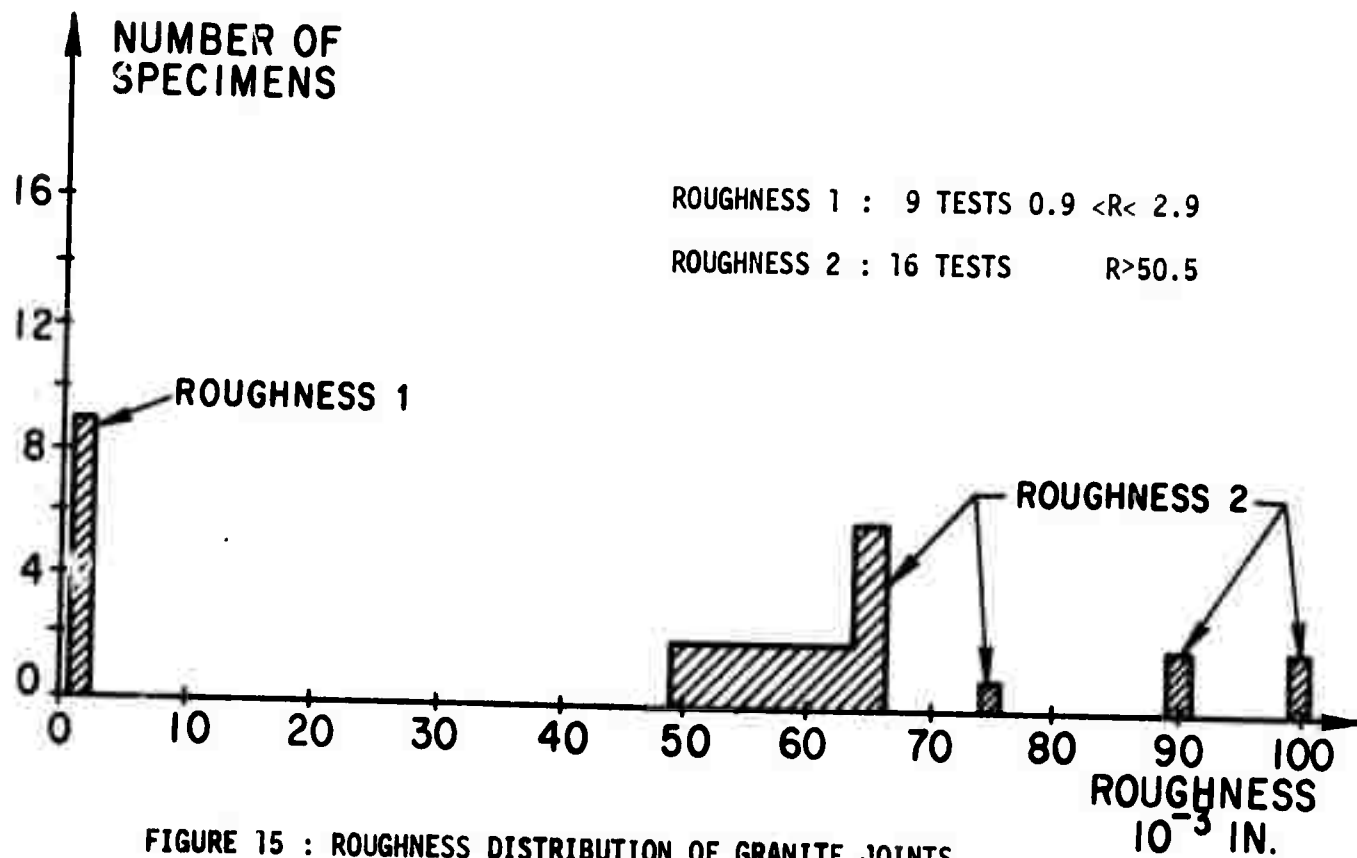


FIGURE 15 : ROUGHNESS DISTRIBUTION OF GRANITE JOINTS

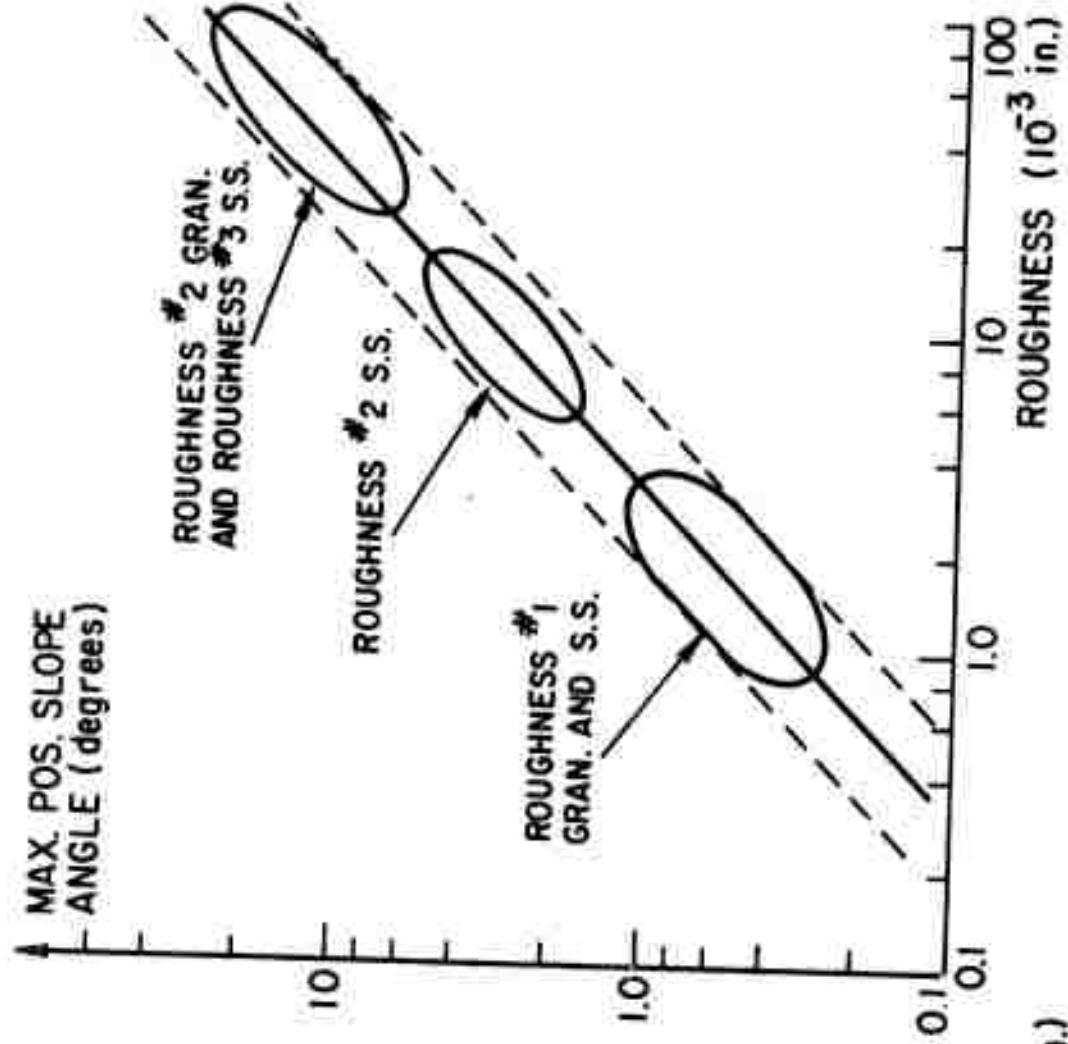
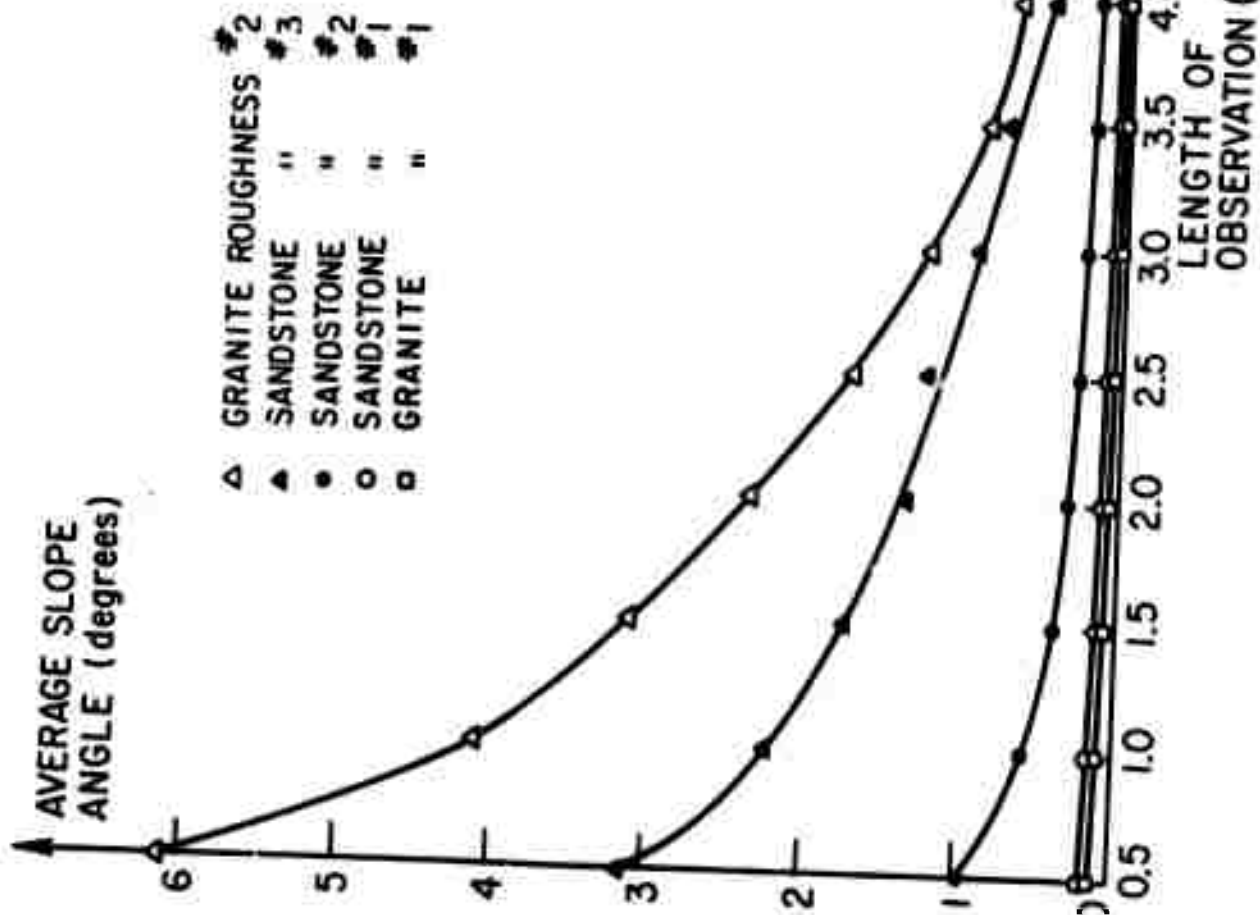


FIGURE 16

FIGURE 17

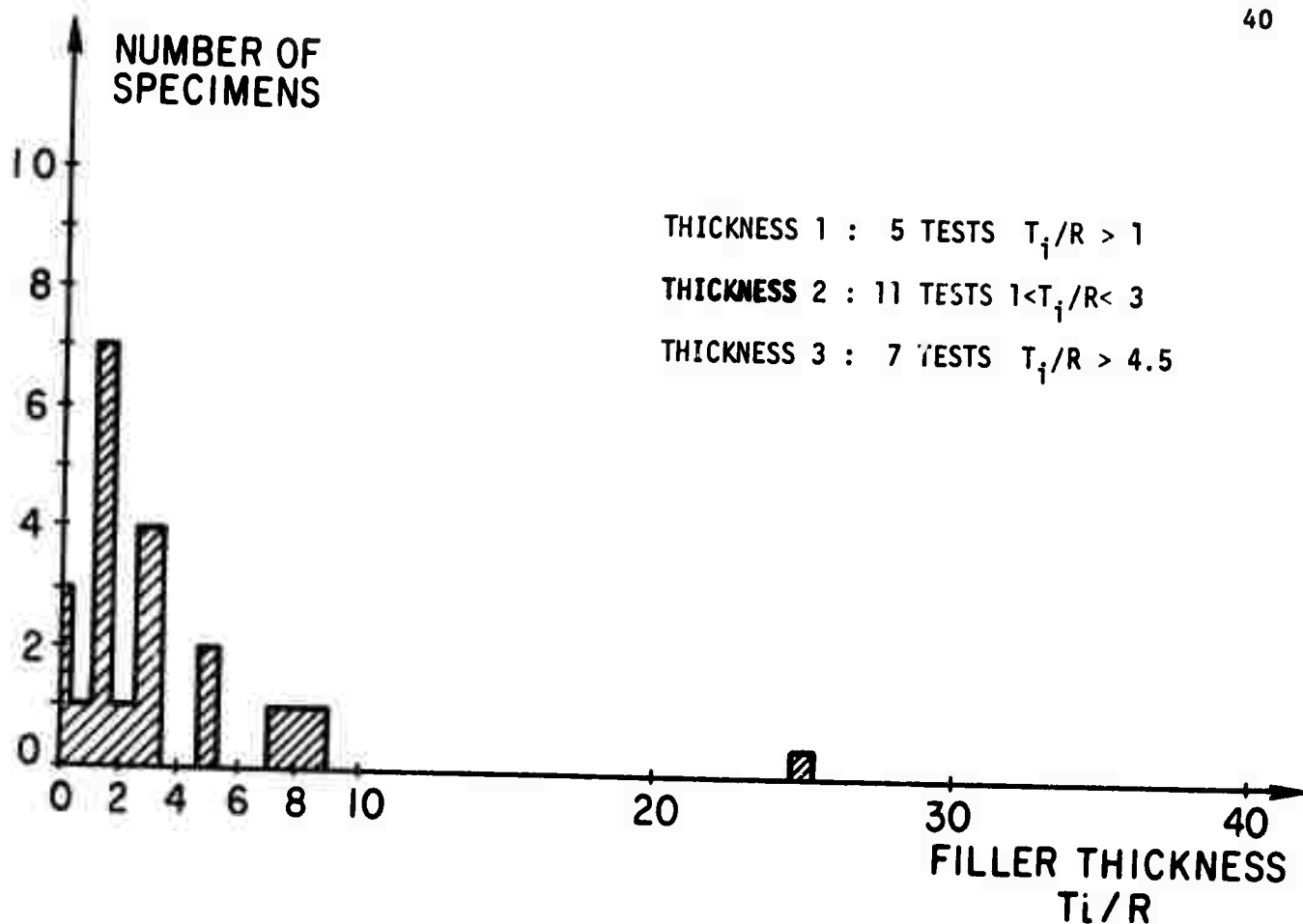


FIGURE 18 : DIMENSIONLESS FILLER THICKNESS (T_f/R) FOR SANDSTONE JOINTS

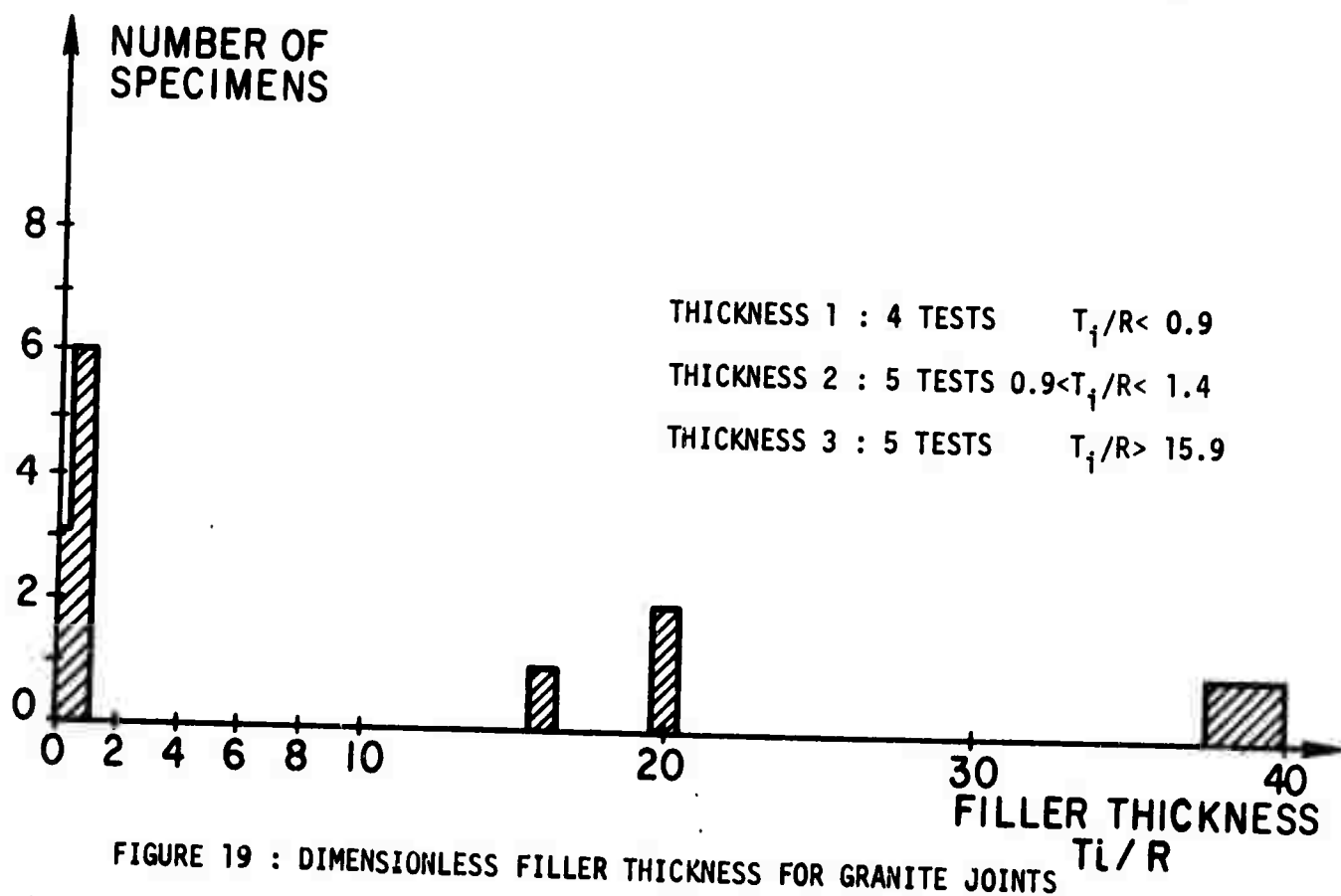


FIGURE 19 : DIMENSIONLESS FILLER THICKNESS FOR GRANITE JOINTS

PART IV: DISCUSSION OF THE TEST RESULTS

The three groups of properties subject to discussion are: 1) the deformability parameters: K_{ss} , u_p and δ , 2) the strength parameters: τ_p , τ_r and 3) the water pressures P , p_1 , p_2 . The values observed are analyzed in terms of their variation as a function of the variables in the testing program, namely:

The normal pressure, σ_n .

The joint filler thickness, T_1 or T_1/R .

The shear rate, $\dot{\tau}$.

The back pressure, P .

The roughness, R .

1. DISCUSSION OF JOINT DEFORMABILITY

a. Sandstone Joints

Shear stiffness: K_{ss}

- increases with increasing σ_n for dry and wet tests
- no pattern for filled tests
- fairly insensitive to T_1/R except at high values (say >10)
- appears to decrease when shear rate $\dot{\tau}$ increases
- fairly insensitive to R in dry and wet tests except at high values say $R > 25 \cdot 10^{-3}$
- appears to increase with increasing P_b in non-filled tests. Not conclusive for filled joints.

Shear displacement at peak: u_p

- increases with σ_n in all tests (ploughing). The effect is less felt on filled joints, and the absolute value of u_p is smaller with filled joints.
- increases slightly with increasing roughness (dry tests)
- the travel to u_p amounts to several times the roughness. Many

asperities must be sheared before reaching the peak.

- in wet tests u_p is almost independent of R except at low pressures (≈ 100 psi).
- insensitive to T_1/R (T_1/R was < 18)
- may increase slightly with higher shear rate
- may increase slightly with higher P_b

σ_n overshadows every other parameter for influence on u_p .

Dilatancy angle: δ

Roughness 3 is not a natural roughness. It will give a contraction in most cases ($\delta < 0$). Eliminating tests with roughness 3 it appears that even at high values of R (up to 45×10^{-3}), δ stays small in this weak rock ($< 4^\circ$). (dry tests). In wet tests, and for roughness 4 there is a strong decrease of δ with σ_n . For wet or filled tests the no-dilatation pressure is below 500 psi, whatever the roughness. For filled joints it takes a very large T_1/R (> 20) to influence δ . The primary factor is R .

b. Granite Joints

Shear stiffness: K_{ss}

- increases with σ_n in wet tests
- effect of R is not conclusive except at high values ($R > 70 \times 10^{-3}$) where K_{ss} increases T_1/R . This increase in K_{ss} can be accompanied by lower strength; joints with high T_1/R can have high K_{ss} and low strength.
- effect of $\dot{\tau}$ is not conclusive
- in wet tests K_{ss} seems to increase markedly with higher P_b
- this is not exhibited in filled tests.

Shear displacement at peak: u_p

- increases with higher σ_n (wet tests)
- seems to decrease when R increases
- the values of u_p are comparable to those for sandstone everything else

being equal

- results of filled tests are not conclusive here, for the influence of σ_n or T_1/R , or P_b
- results are not conclusive for the influence of $\dot{\tau}$
- u_p would seem to become smaller when P_b increases; under higher P_b the peak is reached sooner (in wet tests).

Dilatancy angle: δ

Wet tests:

- the primary factor is again R
- below $\sigma_n = 1,500$ psi and for large roughnesses, δ is not sensitive to σ_n
- the no-dilatancy pressure is in excess of 1,500 psi

Filled tests:

- filled joints do not dilate at $\sigma_n = 1,500$ psi, irrespective of joint roughness.

For the reader's convenience the previous conclusions are condensed in table 7.

2. DISCUSSION OF JOINT STRENGTH

The strength of the joint specimens will be discussed with reference to points plotted in the (τ, σ) plane. Figure 20 shows peak shear stress (τ_p) versus σ for all tests with dry and wet sandstone while figure 21 shows residual strength τ_r versus σ for the same tests. The roughness, in 10^{-3} inches, is given beside each (τ, σ) point. Lines at 28° , 34° , and 43° from the origin have been shown as guides for reference. There is considerable scatter about these lines. The following comments derive from figures 20 and 21. Peak and residual strengths are about the same for the sandstone. The sandblasted specimens (roughness 2) show the lowest strengths of the three roughness groups; this method of rough joint production is unsatisfactory for unfilled joints as the halves of the specimen do not mate. Water raises

the strength slightly. Whether this is a true antilubrication effect or an apparent effect contained within the scatter band is not definite.

The roughest specimens, produced by splitting (roughness 3), display evidence of a downward bend in the strength curve; a bend is shown at σ_p equal to about 600 psi. However the data are insufficient to definitively compare confidence limits for straight versus curved strength lines. The saw cut surfaces always give $\phi = 34^\circ$ which can therefore be accepted as the friction angle (ϕ_μ) for the sandstone.

Peak and residual shear strength data for tests with wet, unfilled joints in granite are given in figures 22 and 23 respectively. There is little difference between peak and residual strength for the specimens with slight roughness produced by diamond sawing; the friction angle ϕ_μ equals 35° . The rough specimens produced by splitting have peak and residual strengths considerably stronger by virtue of geometric effects.

Figure 24 presents strength data for tests on clay-filled joints in granite and sandstone. The strength curve for filling material alone is shown by the dashed line; it was derived from tests with a large ratio of clay thickness to joint roughness (T_f/R). The tests with very thin filling show augmented strength by virtue of the geometric affect of the rough walls. As its thickness is increased, clay filling reduces this strength to that of filling material alone. The wall rock ceases to exert an influence on the joint strength when (T_f/R) becomes greater than about 3. Because of scatter in results, attempts to quantify the results further would be ill-founded until more are obtained. It is important to note, however, that the gouge effect on strength revealed by these data is very significant, as it changes rock mass strength by as much as a factor of 4.

3. DISCUSSION OF WATER PRESSURE RESULTS

In a program of direct shear tests on marl-filled seams, Coyne and Bellier experienced difficulty in obtaining a uniform degree of saturation if the field moisture content was not preserved. With this in mind we designed a system to apply back pressure to theunjacketed specimens; any variability in results deriving from incomplete saturation could then be removed by raising the back pressure sufficiently high. The system can hold up to 700 psi chamber pressure. That the results showed insensitivity to back pressure level demonstrates that complete saturation was not elusive in this program.

The more significant water pressure variable investigated is the joint water pressure induced during shearing without drainage. During a test of a rough joint at low confining pressure, dilation generally occurs. The increasing volume of the dilating joint would be responded by water flow from the chamber into the joint; since flow is retarded by the restricted joint permeability, a negative water pressure transient should develop. Converseley, under high normal pressure where contractancy occurs, a transient water pressure increase should occur. Since the specimens were not jacketed the full pressure buildup would not be measured unless very rapid loading were obtained - i.e. peak loading in a time increment smaller than the time for a pressure pulse to transit the specimen. In this program, such loading rates were not attained and large pressure buildups were not measured. However the sign of induced water pressures consistently followed the above geometric effects, as shown by a comparison of table 6 (column 2) and table 4 (extreme right column). Dilating specimens showed pore pressure decrease of up to 6 psi. Contracting specimens show pore pressure buildup of up to 25 psi. As noted earlier, these pressure indications may be less than the actual pressure peaks in the joint; only two places in the joint were sampled by the piezometers. In the tests currently underway with jacketed specimens, larger pressures are

being observed.

Superimposed on the geometric effect described above one can expect a particle rearrangement effect in the clay of the filler material. Since remoulded clay filler was used, pore pressure buildup from this source was not found. Tests with a filler which undergoes structural collapse on shearing, such as porous plaster and preconsolidated clay are planned in the continuation of this program.

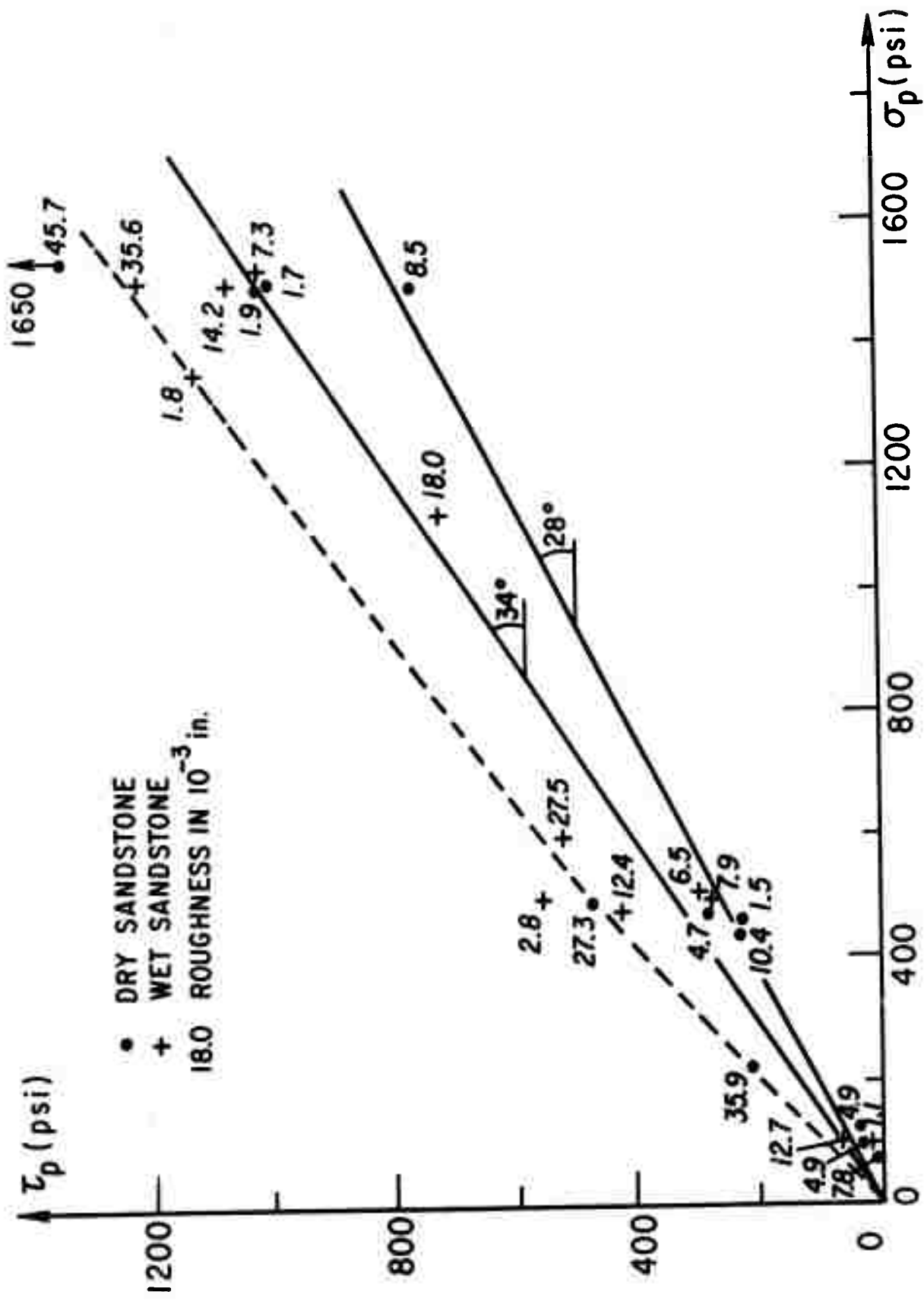


FIGURE 20 : PEAK STRENGTH OF SANDSTONE SPECIMENS

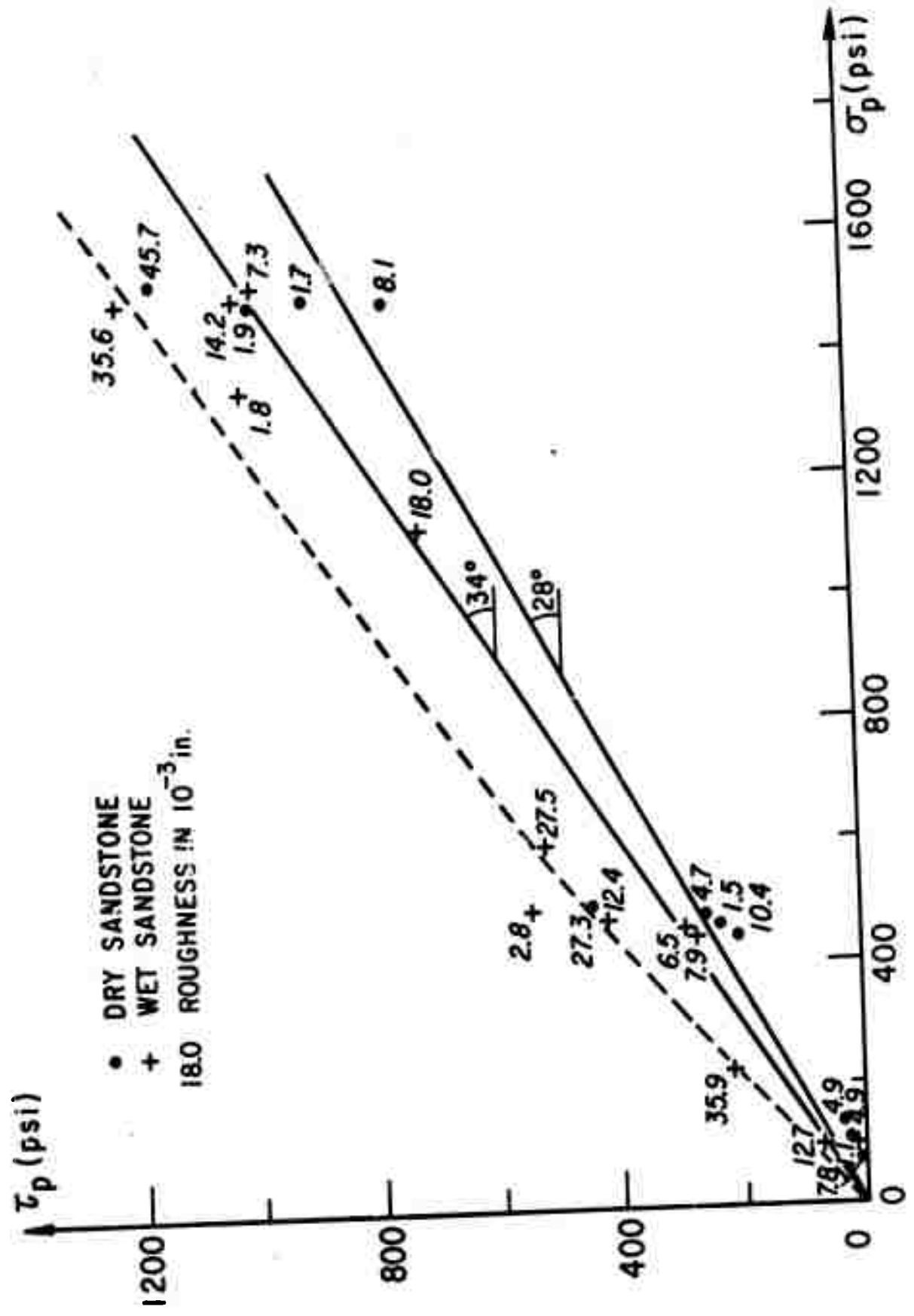


FIGURE 21 : RESIDUAL STRENGTH OF SANDSTONE SPECIMENS

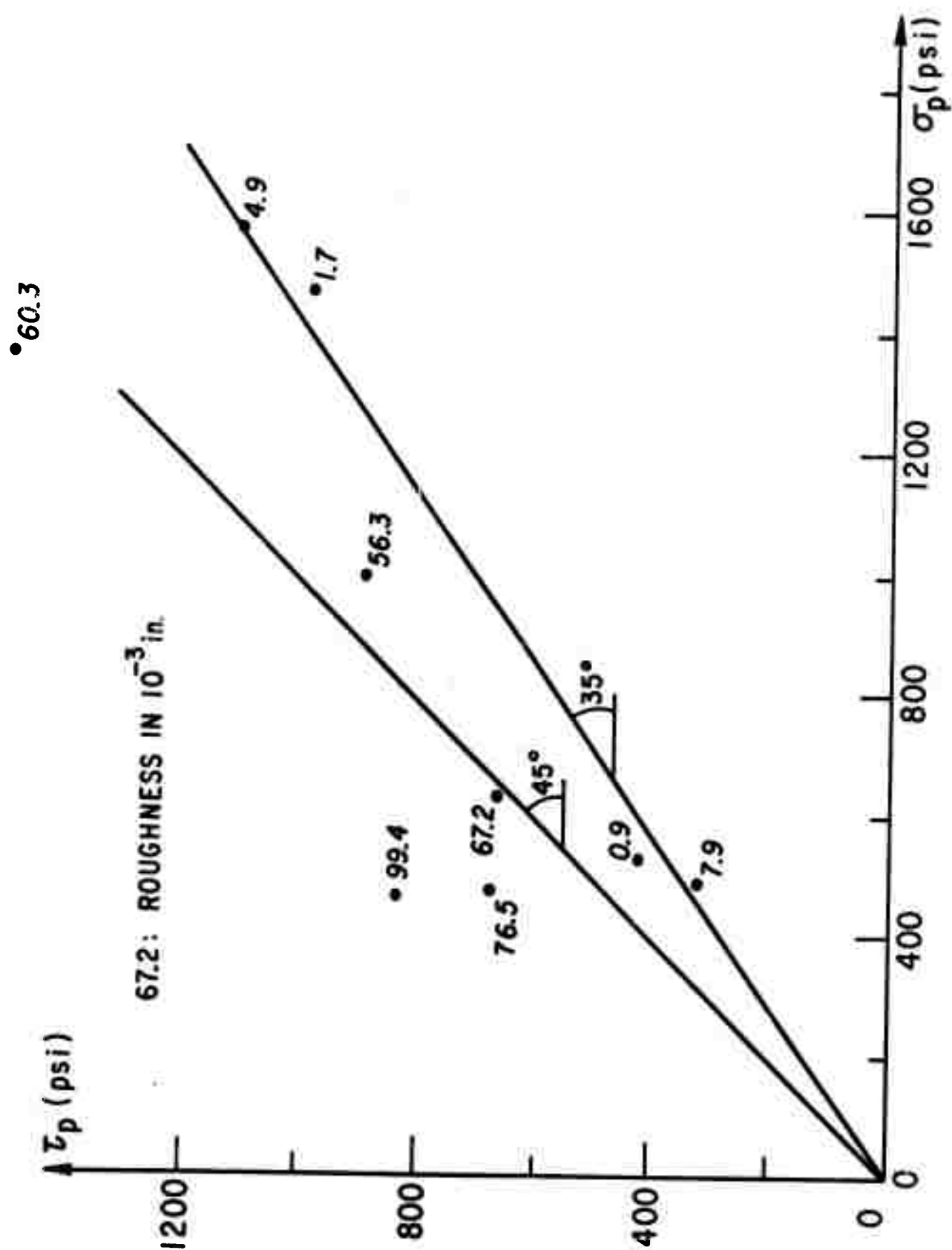


FIGURE 22 : PEAK STRENGTH OF WET GRANITE SPECIMENS

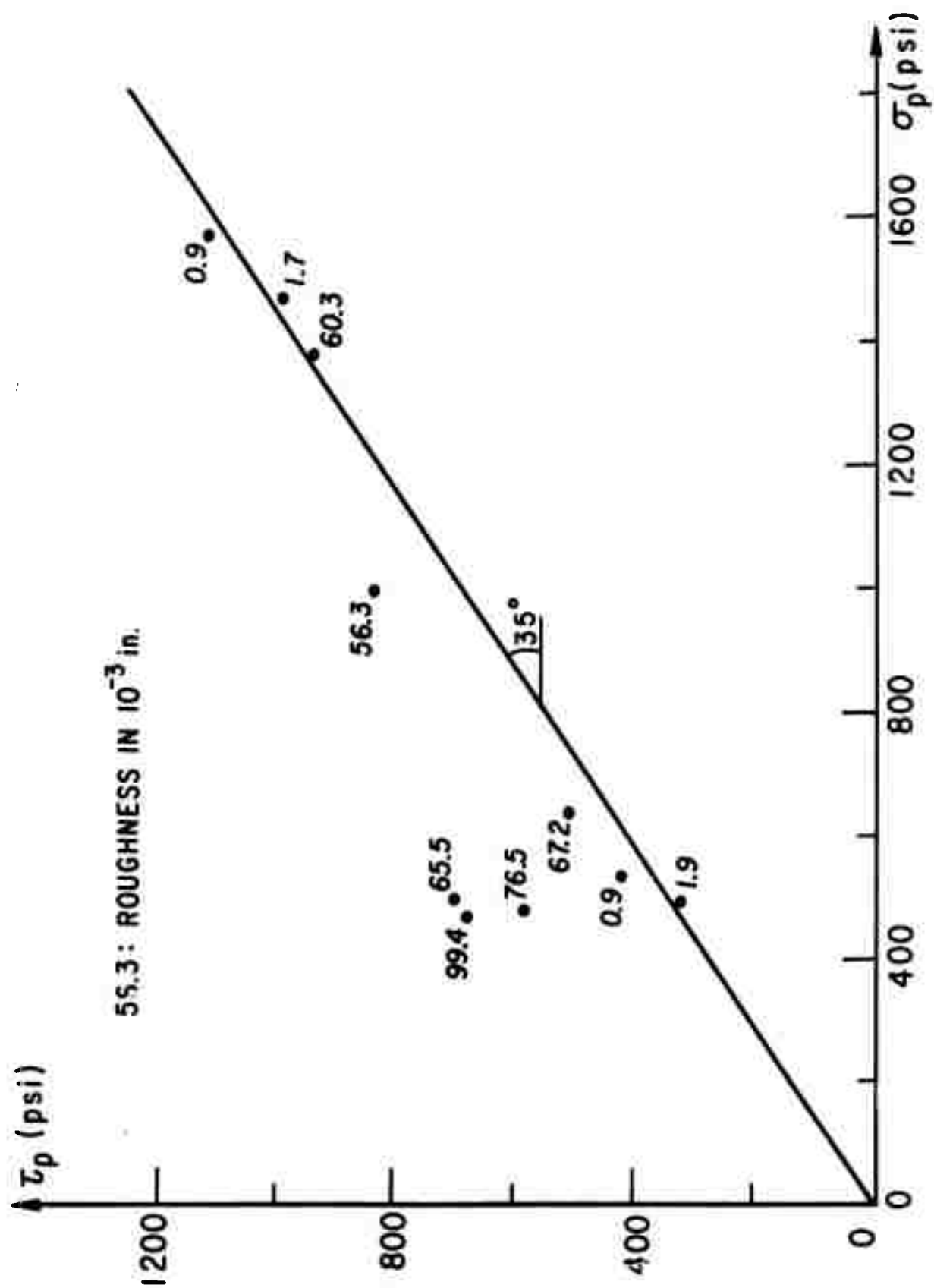


FIGURE 23 : RESIDUAL STRENGTH OF WET GRANITE

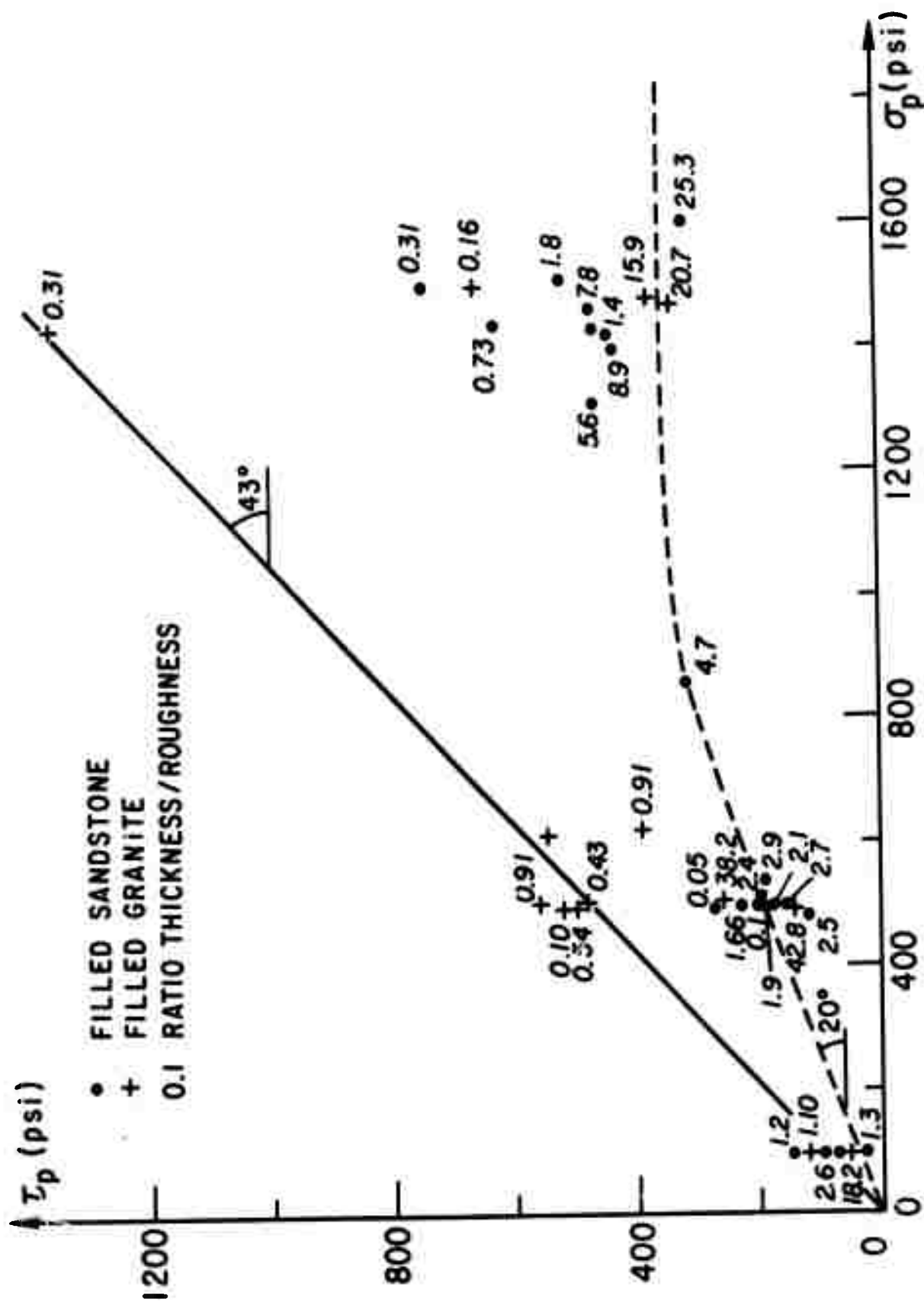


FIGURE 24: STRENGTH DATA FOR CLAY FILLED JOINTS

PART V: SUMMARY-CONCLUSIONS

A program of direct shear tests on samples of rock joints was initiated to gain an improved picture of the deformation and strength of jointed rock masses under load. The shear testing machine, developed under an NSF grant, and improved during this project, allows water pressure to be monitored in the joint plane during shearing. Seventy-two tests were conducted in this first year of an intended 3 year's program; artificial joints were created in two rock types -- granite and sandstone -- with varying wall roughness, filling material thickness, and environmental conditions.

The methods of preparing joint specimens of varying roughness were developed in this project; rough artificial joints were manufactured by splitting the specimens and smooth joints by diamond sawing and lapping. It was difficult to fill the joints to a predetermined thickness with gouge preconsolidated to a desired high normal pressure; remoulded gouge was therefore introduced. Roughness measurements were made and statistical parameters of roughness and waviness were computed using two specially written programs to be found in Appendices B and C. Typical test records are also given in the Appendix.

Table 7 summarizes the sensitivity of deformability and strength parameters to the variables studied. For the sandstone and granite specimens, both peak displacement and joint stiffness varied with normal pressure. The dilation angle decreased rapidly with normal pressure for both rock types and became negative for the sandstone specimens at σ above 500 psi (i.e. the specimens contracted during shear). Induced water pressures measured were not large (<25 psi), possibly due to the problem of sampling water pressures in the joint plane, partly due to the remoulded nature of the filling, and partly because of decay of the water pressure transients in the unjacketed specimens. Dilatant joints generally suffered an increase in pressure while contractant joints underwent a pore pressure buildup. Complete saturation of the joints was obtained, as

evidenced by the insensitivity of the results to chamber back pressure. Filled joints approached the strength of the clay filling material when the thickness was greater than about 3 times the mean roughness amplitude.

Joints and faults exert controls on rock movement below ground and their weakness and deformability limit the "hardness" of underground sites. Furthermore, water pressure phenomena create difficulties for design and construction. This research has added to the technology basis to rational engineering with rock masses. In the work, basic phenomena of jointed rock are being examined experimentally for the first time permitting formulation of correct constitutive laws for joints that are vital to numerical and physical modelling. In continuation, tests with jacketed specimens having preconsolidated filler material are proposed. Experimental methods for these improvements in testing technique have now been developed.

REFERENCES

1. Coulson, J. H. (1970) "The Effect of Surface Roughness on the Shear Strength of Joints in Rocks", Technical Report MRD-270 to U.S. Army Corps of Engineers, Omaha, Nebraska by Dept. of Civil Eng., Univ. of Illinois, Urbana.
2. Fecker, E. and Rengers, N. (1971) "Measurement of Large Scale Roughnesses of Rock Planes by Means of Profilograph and Geological Compass", Proc. Symposium Int. Soc. Rock Mech., Nancy, France, October.
3. Goodman, R. E. (1970) "The Deformability of Joints" in Determination of the In-Situ Modulus of Deformation of Rock, ASTM, Special Techn. Publ. 477, pp. 174-196.
4. Houston, W. N. (1967) "Properties of Kaolinite Clay", Appendix to Ph.D. Dissertation, Geotechnical Engineering, Univ. of California, Berkeley.
5. Kutter, H. K. (1971) "Stress Distribution in Direct Shear Test Samples", Proc. Symposium Int. Soc. Rock Mech., Nancy, France, October.

APPENDIX A

PETROGRAPHY AND MINERALOGY OF THE PROJECT'S ROCK TYPES

(Q. GORTON)

1. PETROGRAPHY OF IMPERVIOUS ROCK SAMPLE

a. Description of Specimen

A block specimen was purchased from a dimension stone quarry near Rocklin, California located on the western flank of the Sierra-Nevada batholith. These mesozoic granitic intrusives range in composition from granite (var. Alaskite) to quartz diorite (tonalite), with quartz monzonite (adamellite) and granodiorite being the most prominent rock types. The quarry is operated within an intrusive body several square miles in extent and mapped as quartz diorite and diorite.

The block specimen appeared sound and unweathered, as judged by fracture through constituent grains on broken surfaces and lack of any discoloration often associated with weathering. It also appeared to be typically isotropic except for the presence of quartz veinlets which traversed the rock in a random fashion at intervals of about one foot. These veinlets, ranging in thickness from .5 to about 2.0 mm, consisted principally of clear quartz with accessory amounts of pyrite. Careful inspection of the rock surface and past experience with such phenomena indicate that the mechanical isotropy is not affected by these apparent discontinuities.

Petrographic examination of the rock both in hand specimen and thin section showed it to be holocrystalline, phaneritic with hypidiomorphic-granular texture.

b. Mineralogical composition

Essential minerals

quartz	clear and unaltered	25%
plagioclase (var. oligoclase)	frequent albite twinning with numerous, narrow lamellae; zoning is apparent from optical characteristics, and selective alteration of calcic rich zones was noted, but the type of zoning (normal, reverse, or oscillatory) was not positively determined.	55%

Accessory minerals

K-feldspar	some Carlsbad twinning present; no zoning observed, but grains were moderately altered, as determined by the degree of pitting.	8%
biotite	pleochroic-yellowish brown to brown	5%
muscovite	non-pleochroic, colorless	4%
hornblende	pleochroic-pale green to green	3%

c. Grain Fabric

The accessory minerals and plagioclase appeared as grains measuring 1 to 3 mm. While the quartz was also represented in this size range, several individuals had dimensions of 10 to 12 mm. Therefore, the rock could be considered as having a poorly developed porphyritic texture, which is significant in that rocks of this composition seldom occur as bonafide porphyries. The rock can be called porphyritic biotite-hornblende quartz diorite (tonalite).

2. PETROGRAPHY OF PERVIOUS ROCK SAMPLE

a. Description of Specimen

A block specimen was purchased from a demolition company in Denver, Colorado, after serving as a large building stone for about a century. The building was typical of those in the old section of Denver, being constructed of red colored dimension stone quarried from the Lyons Sandstone formation. The Lyons Sandstone is a member of the Permian Cassa group and measures 50 to 200 feet thick in its domain of central northern Colorado. The block specimen appeared deteriorated an inch or less from the surface, the remainder being uniformly soft and friable. However, without comparing this sample with the equivalent in-situ formation, it is difficult to determine if the rock is characteristically poorly indurated, or if it has been severely weathered by a century of atmospheric exposure. Although the sample is fairly homogeneous, traces of cross-bedding can be observed, along with less definite indications of bedding or ground water leaching and staining. Even with a block sample, these features are so large scale that they cannot be correctly interpreted without reference to the original outcrop. Preliminary work with the block specimen suggests that this slight expression of fabric does not significantly affect the mechanical isotropy or homogeneity of the rock. Petrographic examination of the rock in both hand specimen and loose grains yielded the following additional information (a thin section was attempted, but the friable nature of the rock prevented proper preparation, using simple methods):

b. Mineralogical Composition

Detrital grains

quartz	clear with surface staining from hematite cement	99%
--------	--------------------------------------------------	-----

Matrix material

iron oxide (hematite)	reddish material coating loose grains, and partially filling the void space between grains	1%
calcite	may have been a co-binder at one time, as evidenced by spotty reactions to dilute acid treatment; however, it is no longer an effective cementing agent either because of in-situ leaching or atmospheric exposure.	trace

c. Grain Fabric

The detrital grains are generally equidimensional (sphericity .8 to .9). They are commonly subrounded with larger individuals rounded and smaller ones subangular (roundness .5 to .8). The grain population appears well sorted with an average size of .10 to .15 mm and a maximum size of about .20 mm. The sandstone is poorly consolidated, exhibiting tangential intergrain contacts, and demonstrates an open pore structure or a potential for high permeability. In conclusion, the rock sample could be best described petrographically as a fine grained quartz sandstone (quartz arenite).

APPENDIX B

ROUGHNESS ANALYSIS PROGRAM , AND

SAMPLE OUTPUT FOR TEST #61

(Y. OHNISHI)


```

000164 TSX1=TSX1*X1(1)+X1(I)
000165 TX12=TX12*X1(1)+X2(I)
000166 TSX2=TSX2*X2(1)+X2(I)
000167 TY=TY+Y(I)
000170 TSY=TSY+Y(I)+Y(I)
000172 TX1Y=TX1Y+X1(I)+Y(I)
000174 TX2Y=TX2Y+X2(I)+Y(I)
000175
000177 30 CONTINUE
000204 A(1,1)=N
000205 A(2,1)=TX1
000206 A(3,1)=TX2
000210 A(2,2)=TSX1
000211 A(3,2)=TX12
000213 A(3,3)=TSX2
000215 A(2,3)=A(3,2)
000216 A(1,3)=A(3,1)
000217 A(1,2)=A(2,1)
000220 L=NP+1
000222 A(1,L)=TY
000223 A(2,L)=TX1Y
000227 A(3,L)=TX2Y
000235 PRINT 249
000240 249 FORMAT(10X,'22HA MATRIX OF NORMAL EQ.,././')
000240 PRINT 250,((A(I,J),J=1,L),I=1,NP)
000257 250 FORMAT(5X,'F15.5')
C
000257 INVERTING A MATRIX
000260 DET=1.0
000262 M=NP+1
000266 I=1
000266 5 PIVOT=A(I,1)
000267 DET=DET*PIVOT
000271 A(I,1)=1.0
000272 J=1
000275 1 A(I,J)=A(I,J)/PIVOT
000301 J=J+1
000303 IF(J.LE.M) GO TO 1
000305 K=1
000306 4 IF(K.EQ.1) GO TO 2
000312 AMULTE=A(K,1)
000313 A(K,1)=0.0
000317 J=1
000326 3 A(K,J)=A(K,J)-AMULTE*A(I,J)
000330 J=J+1
000332 IF(J.LE.M) GO TO 3
000334 2 K=K+1
000336 IF(K.LE.NP) GO TO 4
000337 I=I+1
000340 IF(I.LE.NP) GO TO 5
C
000345 END OF INVERTING A MATRIX
000346 DO 35 I=1,3
000347 R(I)=0.0
000354 35 CONTINUE
000357 DO 40 I=1,NP
000360 R(I)=A(1,L)
000361 40 CONTINUE
000361 SUMYR=0.0
000361 YRMAX=0.0
000361 YRMIN=0.0

```

```

000362 DO 41 I=1,N
000371 YRES=Y(I)-B(1)-B(2)*X1(I)-B(3)*X2(I)
000376 SUMYRE=SUMYRE+YRES
000377 IF (YRES.GE.YRMAX) YRMAX=YRES
000402 IF (YRES.LE.YRMIN) YRMIN=YRES
000406
000407 *1 CONTINUE
000408 YMAXDIF=YRMAX-YRMIN
000411 PRINT 270, YMAX, YRMIN, YMAXDIF
000422 270 FORMAT(5X, 'THE MAX. DIVIATION FROM THE MEAN PLANE', DIRECTION, ' = ', F10.5, '/.//')
000422 1, F10.5, 3X, 'DIRECTION' = F10.5, MAX.DIF, ' = F10.5, /.//')
000430 PRINT 271, SUMYRE
000434 271 FORMAT(5X, 'THE SUM. OF RESIDUALS = ', F15.7, '/.//')
000443 PRINT 299
000443 299 FORMAT(5X, '35 DETERMINED REGRESSION PLANE OR LINE, /')
000454 PRINT 300, (B(I), I=1, NP)
000460 300 FORMAT(5X, 'Y = .2F15.5, X1', F15.5, 'X2', F15.5, '/.//')
000465 SQS IS THE SUM OF SQUARES OF RESIDUALS
000467 SSR IS THE ESTIMATE OF SIGMA SQUARE
000476 SSR=B(2)*(TX1Y-TX1*TY/N)+B(3)*(TX2Y-TX2*TY/N)
000476 ESQ=(TSY-TY*Y/N)-SSR
000476 SQS=ESQ/(N-3)
000476 STORES=SQRT(SQS)
000476 PRINT 500, ESQ, SQS
000476 500 FORMAT(5X, 'THE SUM OF SQUARES OF RESIDUALS = ', F15.5
000476 1, 'THE ESTIMATE OF SIGMA SQUARE = ', F15.5, '/.//')
000476 PRINT 501, STORES
000504 501 FORMAT(5X, 'THE ESTIMATE OF STANDARD DIVIATION OF RESIDUALS = ',
000504 1, F15.7, '/.//')
000504 *** CALCULATION OF DIF. Y(I) DISTRIBUTION ***
000504 TYDIF=0.0
000505 TSYDIF=0.0
000505 SLOPOS=0.0
000506 SLONEG=0.0
000506 M1=0
000507 M2=0
000507 N1=N-NX2
000512 DO 50 I=1,N1
000514 TYDIF=TYDIF+YDIF(I)
000515 TSYDIF=TSYDIF+YDIF(I)*YDIF(I)
000517 IF (YDIF(I)) 53, 52, 51
000521 51 M1=M1+1
000523 SLOPOS=SLOPOS+YDIF(I)
000525 52 GO TO 50
000526 53 M2=M2+1
000530 SLONEG=SLONEG+YDIF(I)
000532 50 CONTINUE
000535 YDMEAN=TYDIF/(N1)
000536 STNDIV=SQRT(TSYDIF/(N1)-YDMEAN**2)
000544 SLOPAV=SLOPOS/M1
000546 SLONAV=SLONEG/M2
000551 PRINT 550, SLOPAV
000556 550 FORMAT(5X, 'THE AVERAGE OF SLOPE OF POSITIVE DIRECTION = ', F10.5, '/.//')
000556 551 PRINT 551, SLONAV
000564 551 FORMAT(5X, 'THE AVERAGE OF SLOPE OF NEGATIVE DIRECTION = ', F10.5, '/.//')
000564 PRINT 601, YDMEAN
000572 501 FORMAT(5X, 'THE MEAN VALUE OF DISTRIBUTION OF SLOPE OR GRADIENT
000572 1 = ', F15.7, '/.//')
000572 PRINT 602, STNDIV

```

```

000600      602 FORMAT(SX, * THE STANDARD DIVIATION OF DISIRIBUTION OF SLOPE
000600      1 OH GRADIENT = *.F15.7,/)
000600      STOP
000602      END

```

PROGRAM LENGTH INCLUDING I/O BUFFERS

```

006043

```

FUNCTION ASSIGNMENTS

STATEMENT ASSIGNMENTS

Statement	Function	Address	Length	Offset	Index	Mode	Value
1	000274	2	000333	3	000315	4	000307
15	000146	41	000407	50	000533	51	000522
100	000523	101	000614	102	000616	103	000636
200	000660	201	000670	202	000672	203	000636
270	000715	271	000732	299	000740	300	000746
550	001001	551	001011	601	001021	602	001032

BLOCK NAMES AND LENGTHS

```

000234

```

VARIABLE ASSIGNMENTS

Variable	Address	Length	Offset	Index	Mode	Value
A	001712	AMULT	001752	R	001707	DET
I	001730	J	001742	K	001751	L
MH1	001733	M1	001770	M2	001771	N
NX2	000232C01	N1	001772	PIVOT	001750	SLNEAV
SLPOAV	001775	SOS	001762	SSR	001760	STDRES
TSX1	001736	TSX2	001740	TSY	001742	TSYDIF
TX12	001737	TX2	001735	TX2Y	001744	TY
X2	001377	Y	000000C01	YDIF	000121C01	YDMEAN
YRMAX	001754	YRMIN	001755			

START OF CONSTANTS-000605

```

TEMP5--001045

```

```

INDIRECTS-001061

```

ROUTINE COMPILES IN 043500

TEST # 61 - GRANITE FILLED , ROUGHNESS 4

NO. OF OBSERVATIONS = 81 NO. OF COEFF. B(I) = 3

LENGTH OF INTERVAL DX1 = .50000

NO. OF INTERVALS IN THE DIP. OF X1 = 2 NO. OF INTERVALS IN THE DIP. OF X2 = 9

Y(I) X1(I) X2(I) GRADIENT(SLOPE) OF Y(I)

.2731	0.	0.	
.2535	.0500	0.	.0728
.2630	.1000	0.	-.0012
.2273	.1500	0.	-.0552
.2114	.2000	0.	-.0378
.2030	.2500	0.	.1050
.2337	.3000	0.	-.0264
.2304	.3500	0.	.0594
.2223	.4000	0.	.0918
.2500	0.	.0500	
.2520	.0500	.0500	-.0132
.3153	.1000	.0500	.1278
.2035	.1500	.0500	-.2246
.2620	.2000	.0500	.1168
.2073	.2500	.0500	.0838
.3169	.3000	.0500	-.0088
.2753	.3500	.0500	-.0352
.3033	.4000	.0500	.0360
.3331	0.	.1000	
.3133	.0500	.1000	.1544
.2573	.1000	.1000	.1600
.2903	.1500	.1000	-.2964
.2025	.2000	.1000	.0634
.2737	.2500	.1000	-.0276
.2761	.3000	.1000	-.0112
.2632	.3500	.1000	-.0173
.3115	.4000	.1000	.0926
.2032	0.	.1500	
.3230	.0500	.1500	.0903
.3770	.1000	.1500	.0978
.2110	.1500	.1500	-.3312
.2033	.2000	.1500	.1470
.2073	.2500	.1500	.0240
.2732	.3000	.1500	-.0360
.3110	.3500	.1500	.0412
.2725	.4000	.1500	-.0578
.2361	0.	.2000	
.2015	.0500	.2000	.0908
.2000	.1000	.2000	.2510
.3247	.1500	.2000	-.1636

Reproduced from
best available copy.

Reproduced from
best available copy.

.1672	.2000	.2000	-.3150
.3122	.2500	.2000	.2700
.2477	.3000	.2000	-.1100
.2106	.3500	.2000	-.0638
.2762	.4000	.2000	.1270
.2677	0.	.2500	.2500
.3132	.1500	.2500	.2250
.3094	.1000	.2500	-.1416
.3474	.1500	.2500	.0760
.2409	.2000	.2500	-.2130
.2317	.2500	.2500	.1176
.2104	.3000	.2500	-.1776
.2733	.3500	.2500	.0700
.2363	.4000	.2500	.0916
.2714	0.	.3000	.1402
.3482	.0500	.3000	.0560
.3175	.1000	.3000	-.0072
.3730	.1500	.3000	-.2802
.2533	.2000	.3000	.1314
.3100	.2500	.3000	-.3460
.1335	.3000	.3000	.2474
.2624	.3500	.3000	.0104
.2421	.4000	.3500	-.0142
.3353	0.	.3500	.0576
.2514	.0500	.3500	.1310
.3100	.1000	.3500	.0656
.3122	.1500	.3500	-.2810
.3322	.2000	.3500	-.0248
.2258	.2500	.3500	-.0132
.2192	.3000	.3500	.0576
.3220	.3500	.3500	.0378
.2719	.4000	.4000	.0180
.2720	0.	.4000	.0524
.2510	.0500	.4000	.0196
.3172	.1000	.4000	-.2630
.3170	.1500	.4000	-.1756
.2355	.2000	.4000	.1950
.1772	.2500	.4000	.0814
.2657	.3000	.4000	.0316
.3354	.3500	.4000	
.2512	.4000	.4000	

A TABLE OF RESIDUALS.

31.00000	16.20000	16.15000	22.84440
16.20000	4.59000	3.22000	4.50480
16.15000	3.22000	4.56750	4.62260
THE MAX. DEVIATION FROM THE MEAN PLANE*+ DIRECTION# = .12023 *-DIRECTION# = -.14395*MAX.DIF. = .26408			

THE SUM OF RESIDUALS = .00000000

OFFERED REGR. PLANE OR LINE

Y = .2112 - .04709 X1 .04993 X2

THE SUM OF SQUARES OF RESIDUALS = .20760 THE ESTIMATE OF SIGMA SQUARE = .00266

THE ESTIMATE OF STANDARD DEVIATION OF RESIDUALS = .0515903 THIS IS THE ROUGHNESS

THE AVERAGE OF SLOPE OF POSITIVE DEFLECTION = .10595

THE AVERAGE OF SLOPE OF NEGATIVE DEFLECTION = -.11743

THE MEAN VALUE OF DISTRIBUTION OF SLOPE OR GRADIENT = .0097722

THE STANDARD DEVIATION OF DISTRIBUTION OF SLOPE OR GRADIENT = .1413418

Reproduced from
best available copy.

APPENDIX C

WAVINESS ANALYSIS PROGRAM , AND

SAMPLE OUTPUT FOR TEST #61

(Y. OHNISHI)


```

000073      PROGRAM MAIN (INPUT,OUTPUT)
000074      DIMENSION X(12001),X2(12001), DX(10),MED(8),Y(01172)
000075      INTEGER WORD(2),WORD1
000076      DATA WORD /MISTAY,ANSTOP, /
000077      COMMON V(81),Y(01172),X(1),X2(1),DX(1)
000078      M IS NO. OF OBSERVATIONS
000079      N IS NO. OF COEFF. ALL
000080      DX(1) IS A LENGTH OF INTERVAL HAD WHEN READ
000081      X(1) IS NO. OF INTERVALS IN THE DIR. OF X1
000082      X2(1) IS NO. OF INTERVALS IN THE DIR. OF X2
000083      READ 101,N,M
000084      READ 102,DX(1)
000085      READ 103,X(1),X2(1)
000086      READ 110,DX(1),I=1,N)
000087      READ 201,X(1),X2(1),I=1,N)
000088      READ 106,WORD1
000089      IF (WORD1.EQ.WORD(1)) GO TO 7
000090      IF (WORD1.EQ.WORD(2)) STOP
000091      GO TO 6
000092      7 READ 107,MED
000093      PRINT 109
000094      PRINT 100,MED
000095      PRINT 100,N,DX(1)
000096      READ 301,Y(1),I=1,N)
000097      CALL SUBV
000098      ON 11 GOTO 8
000099      PRINT 400, DX(1)
000100      J=1
000101      M=1
000102      12 MED=M-1)+0.1
000103      MED=0.2
000104      Y(0)=0.2
000105      MED=MED-1
000106      ON 13 GOTO 14,15
000107      Y(0)=Y(1)+Y(0)
000108      CONTINUE
000109      Y(1)=Y(0)+DX(1)/DX(1)
000110      J=J+1
000111      M=M+1
000112      IF (M.GT.M(1)) GO TO 13
000113      IF (M.EQ.0) GO TO 15
000114      M=0
000115      GO TO 12
000116      15 L=0.01+(DX(1)-K)
000117      PRINT 1000, Y(01172),I=1,L)
000118      Y(0)=0
000119      SL(0)=0.0
000120      SL(0)=0.0
000121      Y(0)=0.0
000122      Y(0)=0.0
000123      M=0
000124      42=0
000125      ON 16 GOTO 1
000126

```

Reproduced from
best available copy.

```

000332 IF(YD1(I)) 53,52,51
000334 51 M1=M1+1
000336 SLOPOS=SLOPOS+YD1(I)
000340 52 GO TO 50
000342 53 M2=M2+1
000344 SLONEG=SLONEG+YD1(I)
000346 50 IF(YD1(I).GE.YDMAX) YDMAX=YD1(I)
000348 IF(YD1(I).LE.YDMIN) YDMIN=YD1(I)
000350 16 CONTINUE
000352 IF(M1.EQ.0) M1=123
000354 IF(M2.EQ.0) M2=456
000356 SLOPOS=SLOPOS/M1
000358 SLONEG=SLONEG/M2
000360 SPD=180.0*ATAN(SLOPOS)/3.14
000362 SNO=180.0*ATAN(SLONEG)/3.14
000364 YDADG=180.0*ATAN(YDMAX)/3.14
000366 YDMING=180.0*ATAN(YDMIN)/3.14
000368 PPRINT 550,SLOPOS,SPD
000370 PPRINT 551,SLONEG,SNO
000372 PRINT 2000,YDMAX,YDADG,YDMIN,YDMING
000374 11 CONTINUE
000376 GO TO 6
000378 100 FORMAT(IHO,2X,* NO. OF OBSERVATIONS = *,I10,3X
000380 1,* LENGTH OF INTERVAL HAD BEEN READ,DX1 = *,F10.5,////)
000382 101 FORMAT(2I5)
000384 102 FORMAT(F10.5)
000386 104 FORMAT(2I5)
000388 106 FORMAT(A6)
000390 107 FORMAT(BA9)
000392 108 FORMAT(BA9)
000394 109 FORMAT(IH1)
000396 110 FORMAT(RF5.0)
000398 201 FORMAT(I4F5.2)
000400 101 FORMAT(7F10.5)
000402 400 FORMAT(15X,* WAVELENGTH ON SCALE OF *,F5.2,* INCH *)
000404 550 FORMAT(5X,* THE AVERAGE OF SLOPE OF POSITIVE DIRECTION =*,F10.5,2X
000406 1,* THE AVE. POS. SLOPE ANGLE=*,F6.1,* DEGREES*)
000408 551 FORMAT(5X,* THE AVERAGE OF SLOPE OF NEGATIVE DIRECTION =*,F10.5,2X
000410 1,* THE AVE. NEG. SLOPE ANGLE=*,F6.1,* DEGREES*)
000412 1000 FORMAT(12F10.5)
000414 2000 FORMAT(
000416 1X,* MAX. POS. SLOPE=*,F8.5,2X,* MAX. POS. ANGLE=*,F6.1,2X
000418 1,* MIN. NEG. SLOPE=*,F8.5,2X,* MIN. NEG. ANGLE=*,F6.1,/)
000420 END

```

Reproduced from
best available copy.

P111 FORTRAN COMPILER VERSION 2.3 B.2

```
000002 SUBROUTINE SUBY
000003 COMMON YY(9,9),YD(8,9),NX1,NX2,DX1
000004 NN1=NX1-1
000005 DO 111 J=1,NX2
000006 DO 111 I=1,NN1
000007 YD(I,J)=(YY(I+1,J)-YY(I,J))/DX1
000008 111 CONTINUE
000009 RETURN
000010 END
```

TEST # 61 - GRANITE FILLED , ROUGHNESS 4

NO. OF OBSERVATIONS =	81	LENGTH OF INTERVAL HAD BEEN READ, DX1 =	.50000
MAVINESS ON SCALE OF 1.00 INCH			
07293	-.00120	-.03280	.10900
08490	-.00880	-.03920	.16440
09083	-.00780	-.03170	.14780
07033	-.01490	-.06380	.22500
15823	-.06700	-.00720	.13360
32493	-.01320	-.05760	.08780
THE AVERAGE OF SLOPE OF POSITIVE DIRECTION =			
THE AVERAGE OF SLOPE OF NEGATIVE DIRECTION =			
MAX. POS. SLOPE = 27000 MAX. POS. ANGLE = 15.1			
MAVINESS ON SCALE OF 1.00 INCH			
03590	-.02870	-.04600	.03930
02200	-.00040	-.16670	-.10400
08590	-.00500	-.00360	-.03830
03280	-.06850	-.04770	-.03000
13060	-.04370	-.12180	-.11070
00920	-.13820	-.05650	
THE AVERAGE OF SLOPE OF POSITIVE DIRECTION =			
THE AVERAGE OF SLOPE OF NEGATIVE DIRECTION =			
MAX. POS. SLOPE = .17090 MAX. POS. ANGLE = 9.7			
MAVINESS ON SCALE OF 1.50 INCH			
00513	-.03007	.00533	.01527
01233	-.01300	-.07853	.01653
05907	-.07620	-.06987	-.05467
06900	-.06713	-.04467	-.15693
03300	.00300	-.07333	-.01487
THE AVERAGE OF SLOPE OF POSITIVE DIRECTION =			
THE AVERAGE OF SLOPE OF NEGATIVE DIRECTION =			
MAX. POS. SLOPE = .10267 MAX. POS. ANGLE = 5.9			
MAVINESS ON SCALE OF 2.00 INCH			
00435	-.00370	-.00260	.02630
06170	.00795	.00900	-.00130
05355	-.01340	-.04025	-.04925
01630	-.06495	-.06710	.02685
THE AVERAGE OF SLOPE OF POSITIVE DIRECTION =			
THE AVERAGE OF SLOPE OF NEGATIVE DIRECTION =			
MAX. POS. SLOPE = .05745 MAX. POS. ANGLE = 3.3			
MAVINESS ON SCALE OF 2.50 INCH			
01752	-.00232	.00980	.03940
00584	-.01912	-.03064	.02424
THE AVERAGE OF SLOPE OF POSITIVE DIRECTION =			
THE AVERAGE OF SLOPE OF NEGATIVE DIRECTION =			
MAX. POS. SLOPE = .02644 MAX. POS. ANGLE =			
MAVINESS ON SCALE OF 3.00 INCH			
00435	-.00370	-.00260	.02630
06170	.00795	.00900	-.00130
05355	-.01340	-.04025	-.04925
01630	-.06495	-.06710	.02685
THE AVERAGE OF SLOPE OF POSITIVE DIRECTION =			
THE AVERAGE OF SLOPE OF NEGATIVE DIRECTION =			
MAX. POS. SLOPE = .05745 MAX. POS. ANGLE = 3.3			
MAVINESS ON SCALE OF 3.50 INCH			
00435	-.00370	-.00260	.02630
06170	.00795	.00900	-.00130
05355	-.01340	-.04025	-.04925
01630	-.06495	-.06710	.02685
THE AVERAGE OF SLOPE OF POSITIVE DIRECTION =			
THE AVERAGE OF SLOPE OF NEGATIVE DIRECTION =			
MAX. POS. SLOPE = .05745 MAX. POS. ANGLE = 3.3			
MAVINESS ON SCALE OF 4.00 INCH			
00435	-.00370	-.00260	.02630
06170	.00795	.00900	-.00130
05355	-.01340	-.04025	-.04925
01630	-.06495	-.06710	.02685
THE AVERAGE OF SLOPE OF POSITIVE DIRECTION =			
THE AVERAGE OF SLOPE OF NEGATIVE DIRECTION =			
MAX. POS. SLOPE = .05745 MAX. POS. ANGLE = 3.3			
MAVINESS ON SCALE OF 4.50 INCH			
00435	-.00370	-.00260	.02630
06170	.00795	.00900	-.00130
05355	-.01340	-.04025	-.04925
01630	-.06495	-.06710	.02685
THE AVERAGE OF SLOPE OF POSITIVE DIRECTION =			
THE AVERAGE OF SLOPE OF NEGATIVE DIRECTION =			
MAX. POS. SLOPE = .05745 MAX. POS. ANGLE = 3.3			
MAVINESS ON SCALE OF 5.00 INCH			
00435	-.00370	-.00260	.02630
06170	.00795	.00900	-.00130
05355	-.01340	-.04025	-.04925
01630	-.06495	-.06710	.02685
THE AVERAGE OF SLOPE OF POSITIVE DIRECTION =			
THE AVERAGE OF SLOPE OF NEGATIVE DIRECTION =			
MAX. POS. SLOPE = .05745 MAX. POS. ANGLE = 3.3			
MAVINESS ON SCALE OF 5.50 INCH			
00435	-.00370	-.00260	.02630
06170	.00795	.00900	-.00130
05355	-.01340	-.04025	-.04925
01630	-.06495	-.06710	.02685
THE AVERAGE OF SLOPE OF POSITIVE DIRECTION =			
THE AVERAGE OF SLOPE OF NEGATIVE DIRECTION =			
MAX. POS. SLOPE = .05745 MAX. POS. ANGLE = 3.3			
MAVINESS ON SCALE OF 6.00 INCH			
00435	-.00370	-.00260	.02630
06170	.00795	.00900	-.00130
05355	-.01340	-.04025	-.04925
01630	-.06495	-.06710	.02685
THE AVERAGE OF SLOPE OF POSITIVE DIRECTION =			
THE AVERAGE OF SLOPE OF NEGATIVE DIRECTION =			
MAX. POS. SLOPE = .05745 MAX. POS. ANGLE = 3.3			
MAVINESS ON SCALE OF 6.50 INCH			
00435	-.00370	-.00260	.02630
06170	.00795	.00900	-.00130
05355	-.01340	-.04025	-.04925
01630	-.06495	-.06710	.02685
THE AVERAGE OF SLOPE OF POSITIVE DIRECTION =			
THE AVERAGE OF SLOPE OF NEGATIVE DIRECTION =			
MAX. POS. SLOPE = .05745 MAX. POS. ANGLE = 3.3			
MAVINESS ON SCALE OF 7.00 INCH			
00435	-.00370	-.00260	.02630
06170	.00795	.00900	-.00130
05355	-.01340	-.04025	-.04925
01630	-.06495	-.06710	.02685
THE AVERAGE OF SLOPE OF POSITIVE DIRECTION =			
THE AVERAGE OF SLOPE OF NEGATIVE DIRECTION =			
MAX. POS. SLOPE = .05745 MAX. POS. ANGLE = 3.3			
MAVINESS ON SCALE OF 7.50 INCH			
00435	-.00370	-.00260	.02630
06170	.00795	.00900	-.00130
05355	-.01340	-.04025	-.04925
01630	-.06495	-.06710	.02685
THE AVERAGE OF SLOPE OF POSITIVE DIRECTION =			
THE AVERAGE OF SLOPE OF NEGATIVE DIRECTION =			
MAX. POS. SLOPE = .05745 MAX. POS. ANGLE = 3.3			
MAVINESS ON SCALE OF 8.00 INCH			
00435	-.00370	-.00260	.02630
06170	.00795	.00900	-.00130
05355	-.01340	-.04025	-.04925
01630	-.06495	-.06710	.02685
THE AVERAGE OF SLOPE OF POSITIVE DIRECTION =			
THE AVERAGE OF SLOPE OF NEGATIVE DIRECTION =			
MAX. POS. SLOPE = .05745 MAX. POS. ANGLE = 3.3			
MAVINESS ON SCALE OF 8.50 INCH			
00435	-.00370	-.00260	.02630
06170	.00795	.00900	-.00130
05355	-.01340	-.04025	-.04925
01630	-.06495	-.06710	.02685
THE AVERAGE OF SLOPE OF POSITIVE DIRECTION =			
THE AVERAGE OF SLOPE OF NEGATIVE DIRECTION =			
MAX. POS. SLOPE = .05745 MAX. POS. ANGLE = 3.3			
MAVINESS ON SCALE OF 9.00 INCH			
00435	-.00370	-.00260	.02630
06170	.00795	.00900	-.00130
05355	-.01340	-.04025	-.04925
01630	-.06495	-.06710	.02685
THE AVERAGE OF SLOPE OF POSITIVE DIRECTION =			
THE AVERAGE OF SLOPE OF NEGATIVE DIRECTION =			
MAX. POS. SLOPE = .05745 MAX. POS. ANGLE = 3.3			
MAVINESS ON SCALE OF 9.50 INCH			
00435	-.00370	-.00260	.02630
06170	.00795	.00900	-.00130
05355	-.01340	-.04025	-.04925
01630	-.06495	-.06710	.02685
THE AVERAGE OF SLOPE OF POSITIVE DIRECTION =			
THE AVERAGE OF SLOPE OF NEGATIVE DIRECTION =			
MAX. POS. SLOPE = .05745 MAX. POS. ANGLE = 3.3			
MAVINESS ON SCALE OF 10.00 INCH			
00435	-.00370	-.00260	.02630
06170	.00795	.00900	-.00130
05355	-.01340	-.04025	-.04925
01630	-.06495	-.06710	.02685
THE AVERAGE OF SLOPE OF POSITIVE DIRECTION =			
THE AVERAGE OF SLOPE OF NEGATIVE DIRECTION =			
MAX. POS. SLOPE = .05745 MAX. POS. ANGLE = 3.3			
MAVINESS ON SCALE OF 10.50 INCH			
00435	-.00370	-.00260	.02630
06170	.00795	.00900	-.00130
05355	-.01340	-.04025	-.04925
01630	-.06495	-.06710	.02685
THE AVERAGE OF SLOPE OF POSITIVE DIRECTION =			
THE AVERAGE OF SLOPE OF NEGATIVE DIRECTION =			
MAX. POS. SLOPE = .05745 MAX. POS. ANGLE = 3.3			
MAVINESS ON SCALE OF 11.00 INCH			
00435	-.00370	-.00260	.02630
06170	.00795	.00900	-.00130
05355	-.01340	-.04025	-.04925
01630	-.06495	-.06710	.02685
THE AVERAGE OF SLOPE OF POSITIVE DIRECTION =			
THE AVERAGE OF SLOPE OF NEGATIVE DIRECTION =			
MAX. POS. SLOPE = .05745 MAX. POS. ANGLE = 3.3			
MAVINESS ON SCALE OF 11.50 INCH			
00435	-.00370	-.00260	.02630
06170	.00795	.00900	-.00130
05355	-.01340	-.04025	-.04925
01630	-.06495	-.06710	.02685
THE AVERAGE OF SLOPE OF POSITIVE DIRECTION =			
THE AVERAGE OF SLOPE OF NEGATIVE DIRECTION =			
MAX. POS. SLOPE = .05745 MAX. POS. ANGLE = 3.3			
MAVINESS ON SCALE OF 12.00 INCH			
00435	-.00370	-.00260	.02630
06170	.00795	.00900	-.00130
05355	-.01340	-.04025	-.04925
01630	-.06495	-.06710	.02685
THE AVERAGE OF SLOPE OF POSITIVE DIRECTION =			
THE AVERAGE OF SLOPE OF NEGATIVE DIRECTION =			
MAX. POS. SLOPE = .05745 MAX. POS. ANGLE = 3.3			
MAVINESS ON SCALE OF 12.50 INCH			
00435	-.00370	-.00260	.02630
06170	.00795	.00900	-.00130
05355	-.01340	-.04025	-.04925
01630	-.06495	-.06710	.02685
THE AVERAGE OF SLOPE OF POSITIVE DIRECTION =			
THE AVERAGE OF SLOPE OF NEGATIVE DIRECTION =			
MAX. POS. SLOPE = .05745 MAX. POS. ANGLE = 3.3			
MAVINESS ON SCALE OF 13.00 INCH			
00435	-.00370	-.00260	.02630
06170	.00795	.00900	-.00130
05355	-.01340	-.04025	-.04925
01630	-.06495	-.06710	.02685
THE AVERAGE OF SLOPE OF POSITIVE DIRECTION =			
THE AVERAGE OF SLOPE OF NEGATIVE DIRECTION =			
MAX. POS. SLOPE = .05745 MAX. POS. ANGLE = 3.3			
MAVINESS ON SCALE OF 13.50 INCH			
00435	-.00370	-.00260	.02630
06170	.00795	.00900	-.00130
05355	-.01340	-.04025	-.04925
01630	-.06495	-.06710	.02685
THE AVERAGE OF SLOPE OF POSITIVE DIRECTION =			
THE AVERAGE OF SLOPE OF NEGATIVE DIRECTION =			
MAX. POS. SLOPE = .05745 MAX. POS. ANGLE = 3.3			
MAVINESS ON SCALE OF 14.00 INCH			
00435	-.00370	-.00260	.02630
06170	.00795	.00900	-.00130
05355	-.01340	-.04025	-.04925
01630	-.06495	-.06710	.02685
THE AVERAGE OF SLOPE OF POSITIVE DIRECTION =			
THE AVERAGE OF SLOPE OF NEGATIVE DIRECTION =			
MAX. POS. SLOPE = .05745 MAX. POS. ANGLE = 3.3			
MAVINESS ON SCALE OF 14.50 INCH			
00435	-.00370	-.00260	.02630
06170	.00795	.00900	-.00130
05355	-.01340	-.04025	-.04925
01630	-.06495	-.06710	.02685
THE AVERAGE OF SLOPE OF POSITIVE DIRECTION =			
THE AVERAGE OF SLOPE OF NEGATIVE DIRECTION =			
MAX. POS. SLOPE = .05745 MAX. POS. ANGLE = 3.3			
MAVINESS ON SCALE OF 15.00 INCH			
00435	-.00370	-.00260	.02630
06170	.00795	.00900	-.00130
05355	-.01340	-.04025	-.04925
01630	-.06495	-.06710	.02685
THE AVERAGE OF SLOPE OF POSITIVE DIRECTION =			
THE AVERAGE OF SLOPE OF NEGATIVE DIRECTION =			
MAX. POS. SLOPE = .05745 MAX. POS. ANGLE = 3.3			
MAVINESS ON SCALE OF 15.50 INCH			
00435	-.00370	-.00260	.02630
06170	.00795	.00900	-.00130
05355	-.01340	-.04025	-.04925
01630	-.06495	-.06710	.02685
THE AVERAGE OF SLOPE OF POSITIVE DIRECTION =			
THE AVERAGE OF SLOPE OF NEGATIVE DIRECTION =			
MAX. POS. SLOPE = .05745 MAX. POS. ANGLE = 3.3			
MAVINESS ON SCALE OF 16.00 INCH			
00435	-.00370	-.00260	.02630
06170	.00795	.00900	-.00130
05355	-.01340	-.04025	-.04925
01630	-.06495	-.06710	.02685
THE AVERAGE OF SLOPE OF POSITIVE DIRECTION =			
THE AVERAGE OF SLOPE OF NEGATIVE DIRECTION =			
MAX. POS. SLOPE = .05745 MAX. POS. ANGLE = 3.3			
MAVINESS ON SCALE OF 16.50 INCH			
00435	-.00370	-.00260	.02630
06170	.00795	.00900	-.00130
05355	-.01340	-.04025	-.04925
01630	-.06495	-.06710	.02685
THE AVERAGE OF SLOPE OF POSITIVE DIRECTION =			
THE AVERAGE OF SLOPE OF NEGATIVE DIRECTION =			
MAX. POS. SLOPE = .05745 MAX. POS. ANGLE = 3.3			
MAVINESS ON SCALE OF 17.00 INCH			
00435	-.00370	-.00260	.02630
06170	.00795	.00900	-.00130
05355	-.01340	-.04025	-.04925
01630	-.06495	-.06710	.02685
THE AVERAGE OF SLOPE OF POSITIVE DIRECTION =			
THE AVERAGE OF SLOPE OF NEGATIVE DIRECTION =			
MAX. POS. SLOPE = .05745 MAX. POS. ANGLE = 3.3			
MAVINESS ON SCALE OF 17.50 INCH			
00435	-.00370	-.00260	.02630
06170	.00795	.00900	-.00130
05355	-.01340	-.04025	-.04925
01630	-.06495	-.06710	.02685
THE AVERAGE OF SLOPE OF POSITIVE DIRECTION =			
THE AVERAGE OF SLOPE OF NEGATIVE DIRECTION =			
MAX. POS. SLOPE = .05745 MAX. POS. ANGLE = 3.3			
MAVINESS ON SCALE OF 18.00 INCH			
00435	-.00370	-.00260	.02630
06170	.00795	.00900	-.00130
05355	-.01340	-.04025	-.04925
01630	-.06495	-.06710	.02685
THE AVERAGE OF SLOPE OF POSITIVE DIRECTION =			
THE AVERAGE OF SLOPE OF NEGATIVE DIRECTION =			
MAX. POS. SLOPE = .05745 MAX. POS. ANGLE = 3.3			
MAVINESS ON SCALE OF 18.50 INCH			
00435	-.00370	-.00260	.02630
06170	.00795	.00900	-.00130
05355	-.01340	-.04025	-.04925
01630	-.06495	-.06710	.02685
THE AVERAGE OF SLOPE OF POSITIVE DIRECTION =			
THE AVERAGE OF SLOPE OF NEGATIVE DIRECTION =			
MAX. POS. SLOPE = .05745 MAX. POS. ANGLE = 3.3			
MAVINESS ON SCALE OF 19.00 INCH			
00435	-.00370	-.00260	.02630
06170	.00795	.00900	-.00130
05355	-.01340	-.04025	-.04925
01630	-.06495	-.06710	.02685
THE AVERAGE OF SLOPE OF POSITIVE DIRECTION =			
THE AVERAGE OF SLOPE OF NEGATIVE DIRECTION =			
MAX. POS. SLOPE = .05745 MAX. POS. ANGLE = 3.3			
MAVINESS ON SCALE OF 19.50 INCH			
00435	-.00370	-.00260	.02630
06170	.00795	.00900	-.00130
05355	-.01340	-.04025	-.04925
01630	-.06495	-.06710	.02685
THE AVERAGE OF SLOPE OF POSITIVE DIRECTION =			
THE AVERAGE OF SLOPE OF NEGATIVE DIRECTION =			
MAX. POS. SLOPE = .05745 MAX. POS. ANGLE = 3.3			
MAVINESS ON SCALE OF 20.00 INCH			
00435	-.00370	-.00260	.02630
06170	.00795	.00900	-.00130
05355	-.01340	-.04025	-.04925
01630	-.06495	-.06710	.02685
THE AVERAGE OF SLOPE OF POSITIVE DIRECTION =			
THE AVERAGE OF SLOPE OF NEGATIVE DIRECTION =			
MAX. POS. SLOPE = .05745 MAX. POS. ANGLE = 3.3			
MAVINESS ON SCALE OF 20.50 INCH			
00435	-.00370	-.00260	.02630
06170	.00795	.00900	-.00130
05355	-.01340	-.04025	-.04925
01630	-.06495	-.06710	.02685
THE AVERAGE OF SLOPE OF POSITIVE DIRECTION =			
THE AVERAGE OF SLOPE OF NEGATIVE DIRECTION =			
MAX. POS. SLOPE = .05745 MAX. POS. ANGLE = 3.3			
MAVINESS ON SCALE OF 21.00 INCH			
00435	-.0		

.01604 -.08240 -.04604 -.04192 -.03188 -.01568 -.04036 -.03612 -.02992 .00548 .01128 .01368
 THE AVERAGE OF SLOPE OF POSITIVE DIRECTION = .01914 THE AVE. POS. SLOPE ANGLE = 1.1 DEGREES
 THE AVERAGE OF SLOPE OF NEGATIVE DIRECTION = -.03414 THE AVE. NEG. SLOPE ANGLE = -2.0 DEGREES
 MAX.POS.SLOPE = .03972 MAX.POS.ANGLE = 2.3 MIN.NEG.SLOPE = -.08240 MIN.NEG.ANGLE = -4.7

WAVINESS ON SCALE OF 3.00 INCH

.01020 .00707 .02347 .01463 .01097 -.00433 .01443 -.01593 -.02867 -.00080 -.00907 -.03500
 .01220 -.02357 -.04423 -.01893 -.04313 -.00430 -.04397 -.02737 -.03613 -.02877 -.00347 -.01900
 .00757 .01813 .01457
 THE AVERAGE OF SLOPE OF POSITIVE DIRECTION = .01242 THE AVE. POS. SLOPE ANGLE = .7 DEGREES
 THE AVERAGE OF SLOPE OF NEGATIVE DIRECTION = -.02275 THE AVE. NEG. SLOPE ANGLE = -1.3 DEGREES
 MAX.POS.SLOPE = .02347 MAX.POS.ANGLE = 1.3 MIN.NEG.SLOPE = -.04423 MIN.NEG.ANGLE = -2.5

WAVINESS ON SCALE OF 3.50 INCH

.01723 .01794 .00751 .01454 .00583 -.00043 .00520 -.01603 -.00723 -.00206 -.00483 -.02391
 -.00229 -.02154 -.01643 .00957 .01811 .02006 .01356
 THE AVERAGE OF SLOPE OF POSITIVE DIRECTION = .01053 THE AVE. POS. SLOPE ANGLE = .8 DEGREES
 THE AVERAGE OF SLOPE OF NEGATIVE DIRECTION = -.01053 THE AVE. NEG. SLOPE ANGLE = -.6 DEGREES
 MAX.POS.SLOPE = .02006 MAX.POS.ANGLE = 1.1 MIN.NEG.SLOPE = -.02391 MIN.NEG.ANGLE = -1.4

WAVINESS ON SCALE OF 4.00 INCH

.02655 .01108 .02018 -.03267 .00955 .00720 -.00033 -.00340 .01980
 THE AVERAGE OF SLOPE OF POSITIVE DIRECTION = .01572 THE AVE. POS. SLOPE ANGLE = .9 DEGREES
 THE AVERAGE OF SLOPE OF NEGATIVE DIRECTION = -.00213 THE AVE. NEG. SLOPE ANGLE = -.1 DEGREES
 MAX.POS.SLOPE = .02655 MAX.POS.ANGLE = 1.5 MIN.NEG.SLOPE = -.00340 MIN.NEG.ANGLE = -.2

APPENDIX D

TYPICAL TEST RECORD (TEST # 61)

UNIVERSITY OF CALIFORNIA
ROCK MECHANICS LABORATORY

Direct Shear Test

Date: _____ Accession Number: _____
 Operator: Heuze / Ohnishi Test Series or
 Sponsor: ARPA 1971-1972
 Series Number: # 61

Sample Description

Rock Type GRANITE
 Size 4.75 * 4.75 in.

Discontinuity Description

Type of Joint Filled
 Comment Roughness 4 (Split)

Filling Material Kaolinite (mm) (in)
 Thickness 7.2 * 10⁻² in.
 Preconsolidation pressure 100 psi

Shear Rate #1 (L 50) in/min : 0.1

Back Pressure P_b 200 psi

Normal Pressure at Start of Virgin Shear Test

Accumulator pressure (psi)
 Normal force (lbs)
 Normal stress (psi) 500 psi

ROUGHNESS MEASUREMENTS

Shear Test Number

Test Series

Number in Series

ARPA 1971-1972

61

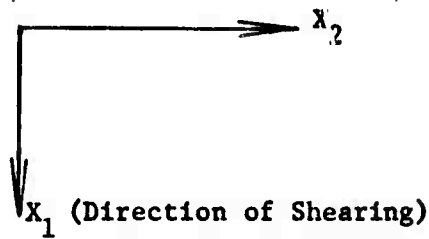
Date

Operator

Grid Size

Heuzé

0.5 in.



.2201	.2595	.2308	.2832	.2361	.2677	.2704	.3055	.2720
.2565	.2529	.3130	.3286	.2815	.3802	.3445	.2584	.2810
.2559	.3168	.3975	.3775	.4070	.3094	.3775	.3489	.3072
.2278	.2045	.2493	.2119	.3247	.3474	.3739	.3822	.3170
.2114	.2629	.2935	.2858	.1672	.2409	.2438	.2382	.2855
.2639	.3078	.2797	.2978	.3022	.2997	.3105	.2258	.1972
.2507	.3034	.2741	.2808	.2427	.2109	.1385	.2192	.2947
.2804	.2858	.2652	.3014	.2108	.2508	.2624	.2480	.3354

.3263 .3038 .3115 .2725 .2743 .2965 .2691 .2919 .3512

Log of Direct Shear Test XYY' Record

Test Accession No.

ARPA 1971-1972 # 61

	<u>Subtest 1 (Reading numbers:)</u>			
	Channel	Name of Variable	Volts/inch	1 inch =:
X	1	σ_n	0.10	2,060 lbs
Y ₁	6	v	0.05	5.63×10^{-3} in.
Y ₂	7	u	0.01	4.0×10^{-3} in.
	<u>Subtest 2 (Reading numbers:)</u>			
			<u>X-Y-Y' #1</u>	<u>X-Y-Y' #2</u>
X	5	P	0.10	P Scale 2
Y ₁	6	v	0.05	p ₁ Scale 2
Y ₂	7	u	0.01	p ₂ Scale 2
	<u>Subtest 3 (Reading numbers:)</u>			
				<u>X-Y-Y' #1</u>
X	2	τ	0.10	2,060 lbs
Y ₁	6	v	0.05	5.63×10^{-3} in.
Y ₂	7	u	0.05	2.0×10^{-2} in.
	<u>Subtest 3 (Reading numbers:)</u>			
				<u>X-Y-Y' #2</u>
X	2	τ	Scale 1	
Y ₁	3	P ₁	Scale 5	
Y ₂	4	P ₂	Scale 5	

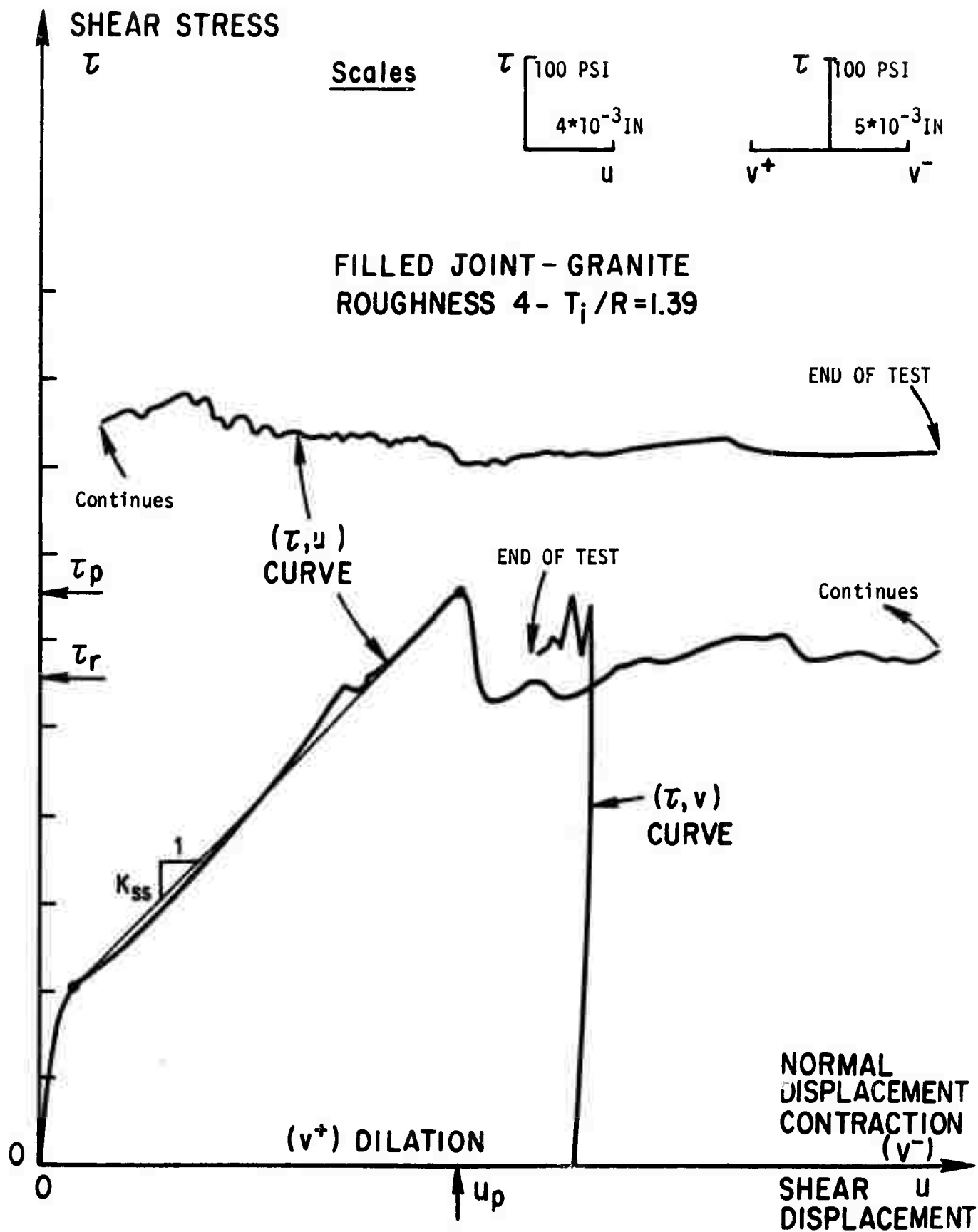


FIGURE 25 : RECORD OF TEST # 61